



# Petrology, Geochemistry and Petrogenetic Aspects of Ediacaran Dokhan Volcanics at Wadi Zareib, Central Eastern Desert, Egypt

Hatem M. El-Desoky<sup>1\*</sup>, Ahmed M. El Mezayen<sup>2</sup> and Akram E. Serag<sup>2</sup>

<sup>1</sup>Department of Geology, Faculty of Sciences, Al-Azhar University, Cairo, Egypt

<sup>2</sup>Ideal Standard Company, Egypt

\*Corresponding author E-mail: [hatem\\_eldesoky@yahoo.com](mailto:hatem_eldesoky@yahoo.com)

Accepted 10 April, 2014

## Abstract

The present study embodies the results of field work and laboratory investigations and attempts to present the geology, petrography, geochemistry and petrogenesis of the Ediacaran Dokhan Volcanics at Wadi Zareib, Central Eastern Desert, Egypt. The investigated area is located along the Red Sea Coast and most common rock types among the Dokhan Volcanics are rhyolites and trachyandesites are commonly interbedded with lava flows successions. Microphenocrysts of quartz, alkali feldspars and plagioclase set in a fine-grained groundmass of microcrystalline to felsitic aggregates of quartz and plagioclase together with chlorite, epidote, sericite and hematite. Major element oxides and trace element data suggest that the trachyandesites are genetically related through crystal fractionation. The trace elements Y, Pb, Cu, Zr and Ga show negative anomalies (enriched) relative to Sr and Ba element. Wadi Zareib Dokhan Volcanics were originated from typical calc-alkaline reflecting the magmatic differentiation of metaluminous to peraluminous magma type. The geochemical trends of major oxides and trace elements of the studied volcanic rock varieties may suggest their co-magmatic nature. The Wadi Zareib Dokhan Volcanics display geochemical characteristics of both orogenic arc-type and anorogenic within-plate environments, suggesting eruption in a transitional "post-collisional tectonic setting. These rocks were derived from a single magma and suffered subsequence fractional crystallization.

**Keywords:** Dokhan Volcanics, geochemistry, Neoproterozoic, petrogenesis, petrography and tectonic setting.

## INTRODUCTION

The Ediacaran Era (635–542 Ma) was a time of erratic climate change and rapidly evolving life (Halverson *et al.*, 2009) coeval with the nascent preservation of low geothermal gradient metamorphic belts (Brown, 2007) that has recently been interpreted as a first-order change in continental collision kinematics (Sizova *et al.*, 2010). This period of change also saw the amalgamation of Gondwana through the closure of a number of large ocean basins and the collision of

a series of separate Australia-scale continents (Collins and Pisarevsky, 2005; Fitzsimons, 2000; Meert and Torsvik, 2003; Meert and Van Der Voo, 1997; Pisarevsky *et al.*, 2008; Tohver *et al.*, 2006). The closure of the Mozambique Ocean, which separated Neoproterozoic India from the Congo–Tanzania–Bangweulu Block, was one of the most extensive of these Gondwana-forming orogens (Collins and Windley, 2002; Dalziel, 1997; Jacobs and Thomas, 2004) and created the East African Orogen (EAO) (Stern, 1994).

The East African Orogen was over 6000 km long in Gondwana. The preserved relics of it range from exhumed high-grade metamorphic belts in Southern India, Madagascar and East Africa (the Mozambique Belt) to greenschist and sub-greenschist facies volcanic, plutonic and sedimentary belts in NE Africa and Arabia (the Arabian–Nubian Shield). Much recent work has illustrated that metamorphism related to the closure of the Mozambique Ocean in southern India and eastern Madagascar was related to an Ediacaran collision between Neoproterozoic India and the Congo–Tanzania–Bangweulu Block (Clark *et al.*, 2009; Collins *et al.*, 2010; Collins *et al.*, 2007; Collins *et al.*, 2003; Thomas *et al.*, 2009) that had previously accreted a continent known as Azania during the Cryogenian (Collins, 2006; Collins and Windley, 2002) to form the Malagasy Orogen (Collins and Pisarevsky, 2005). The Mozambique Ocean suture heads NW from Madagascar into Somalia where it was correlated with the Maydh greenstone belt by Collins and Windley (2002) and into the Arabian Peninsula. This reconstruction is problematic because a number of workers have suggested that the Arabian Nubian Shield was fully amalgamated and connected with the stable Omani basement before 650 Ma. This hypothesis is based on a correlation between the Nafun Group in Oman and Jibalah Group in the eastern ANS and the presence of Cryogenian detrital zircons in Oman that are interpreted as originating in the Arabian–Nubian Shield (Allen, 2007). However, Stern and Johnson (2010) have highlighted important differences between the detrital zircon age distributions of Oman and the ANS.

The basement complex of Egypt in the Eastern Desert and Sinai is a juvenile terrane defined by Neoproterozoic Nd model ages (Stern, 2002). The most conspicuous feature of this terrane is the presence of highly deformed and metamorphosed dismembered ophiolitic suites, volcano-sedimentary successions and calc-alkaline I-type intrusive complexes. Most previous geological studies (Bentor, 1985; Vail, 1985; El Gaby *et al.*, 1988; Kröner *et al.*, 1988; Stern, 1994) reveal an essential role of the convergent processes in the evolution of the Egyptian basement complex. The processes include (1) subduction; (2) accretion of intra-oceanic island arcs, back arc basins and micro-continental plates; followed by (3) crustal thickening (Stern, 1994). These processes evolved during Neoproterozoic Era between about 900 and 614 Ma (Stern and Hedge, 1985; Kröner *et al.*, 1992; Beyth *et al.*, 1994; Stern, 1994). The terminal stage (614–550 Ma) of crustal evolution is characterized by (1) the eruption of the Dokhan Volcanics (El Ramly, 1972; Stern and Hedge, 1985), (2) deposition of molasse-type Hammamat sediments (Grothaus *et al.*, 1979; Akaad and Noweir, 1980), and (3) shallow emplacement of the Younger Granites (El Gaby, 1975).

The Dokhan Volcanics are unmetamorphosed in origin and concluded that the different types of "Gabal Dokhan Volcanic series" were subjected to different agents of metamorphism on the basis of recrystallization of crushed plagioclase phenocrysts (Akaad, 1972). These can be divided into two formations by Ahmed (1983) as follows: (1) The lower Dokhan consisting predominantly of andesitic flow and related pyroclastics; and (2) The upper Dokhan consisting of silicic flows and pyroclastic rocks.

This paper presents new geologic, petrographic, geochemical and petrogenetic data on the Dokhan volcanics of Wadi Zareib, Central Eastern Desert, Egypt (Figure1). These volcanics are widely distributed in the Late Neoproterozoic (Ediacaran) outcropping in the Eastern Desert. This area lies between latitudes 25°49' - 26°08'N and Longitudes 34°10' - 34°20' E, covering about 169 km<sup>2</sup>. Wadi Zareib area lies 5 km to the south Quseir City, on the Quseir-Mersa Alam paved road.

The detailed geology of the Red Sea costal plain is discussed elsewhere (Beadnell, 1924 and Issawi *et al.*, 1971). Sabet (1958) described the geology of the distinct south of the Quseir, along the Red Sea coast. At the base of the Middle Miocene escarpments bordering the open plain, east and west of the basement rocks highlands, Dokhan Volcanics exposures crop out in a NNW-SSE trend along a distance of 10 km. It seems probable that they are localized along a fault forming a fault scarp. There is no contact metamorphism is observed between the Dokhan Volcanics and Middle Miocene coral limestone and limegrit.

## Geologic setting

The basement complex in the Central Eastern Desert displays strong ensimatic affinities and consists mainly of an island arc complex which is overthrust by dismembered ophiolitic sequence and intruded by syntectonic grey granitoides (Stern 1981; Ries *et al.*, 1983; Sturchio *et al.*, 1983; El Ramly *et al.*, 1984). These rock units are overlain by local occurrences of molasse-type Hammamat sediments, Dokhan volcanics and are intruded by post-orogenic younger granites (Grothaus *et al.*, 1979; Greenberg 1981; Ries *et al.*, 1983).

The studied Dokhan Volcanics occur as lava flows and the volcanic varieties are acidic volcanics of rhyolites and trachyandesites.

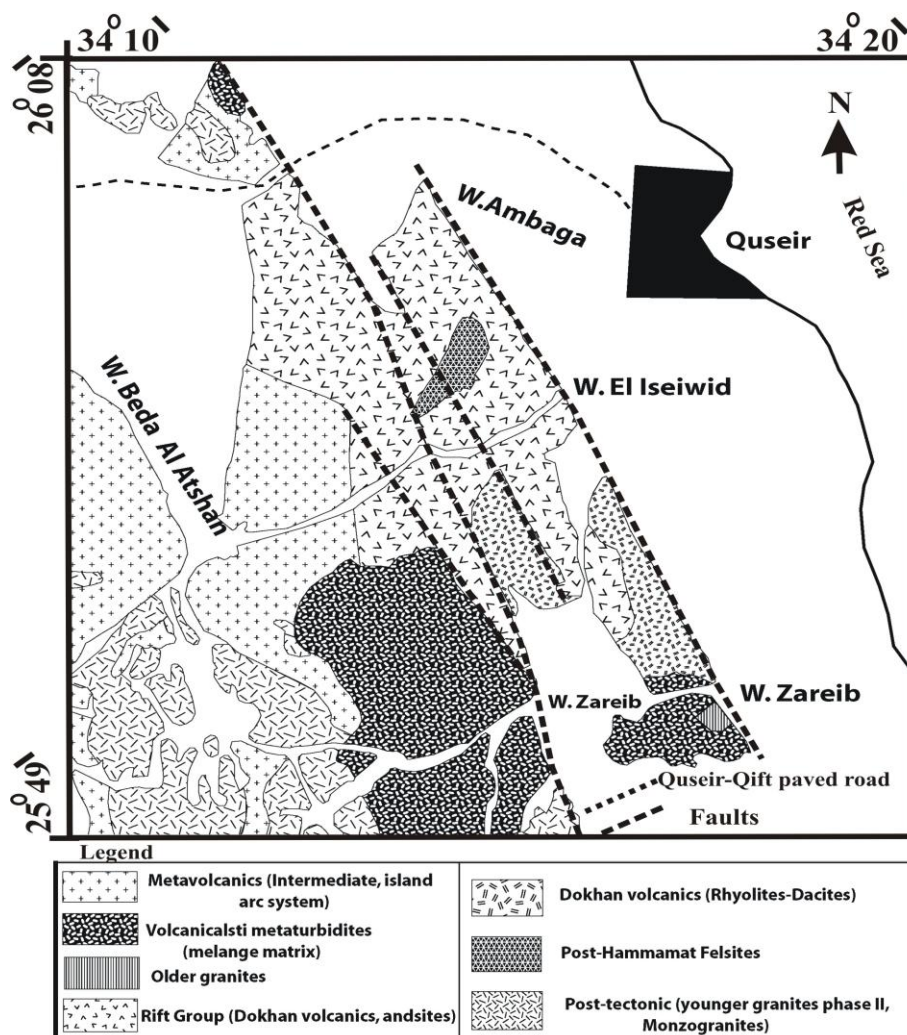


Figure 1. Geological map of Wadi Zareib (Akaad and Abu El-Ela, 2002)

Rhyolites occur as porphyritic lavas and pyroclastics. Phenocrysts of plagioclase, quartz and biotite are present in rhyolites. Rhyolite flows are usually overlying the dark color andesites along Wadi Zareib forming horizontal sheets and flows. In the field, rhyolites are hard, massive and usually characterized by buff or reddish color as the K-feldspar crystals giving their color to the rock. The tuffaceous rhyolite rocks represent the youngest rock type of the Dokhan volcanic group.

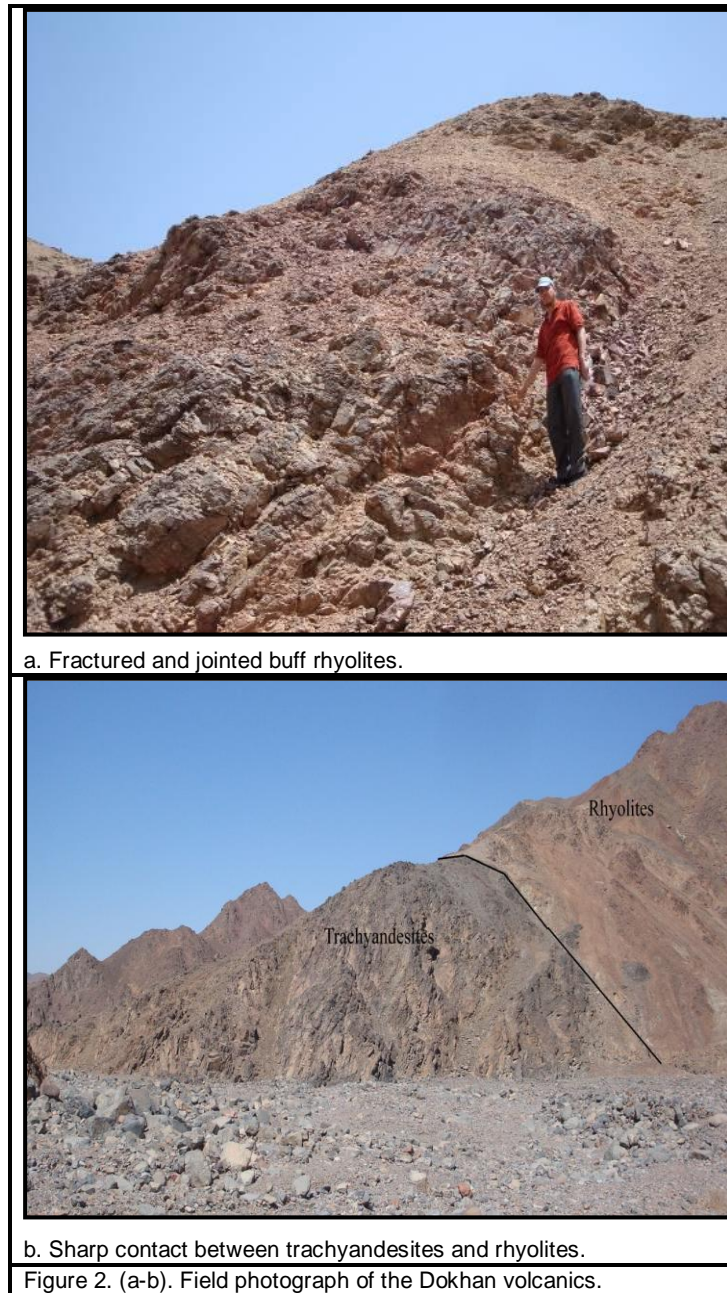
Phenocrysts of quartz (white color) and orthoclase (buff color) characterize the color of rhyolites (Figure 2a). These rocks are massive, fine-grained, light grey and in some places stained by hematite reddish color. Less common rhyolite is massive, very fine-grained, creamy color or has brick red color. Rhyolites are characterized by two sets of jointing; the first is vertical, while the second set is diagonal and trending E-W.

Trachyandesites are commonly porphyritic and relatively grey to blackish grey in color and exhibit phenocrysts of plagioclase set in fine-grained to glassy groundmass. Trachyandesites are well jointed in several directions and fractured into large compact boulders as well as the most common joint directions are 40NW and 20NE (Figure 2b).

### Petrographic Description

Rhyolite is the most abundant rock type in the studied area and consists of microphenocrysts of quartz, alkali feldspars and plagioclase in a fine-grained groundmass of microcrystalline to felsitic aggregates of quartz and plagioclase together with chlorite, epidote, sericite and opaque minerals (Hematite).

Quartz is distinguished as two generations of euhedral and anhedral crystal shape. Euhedral quartz occurs as inclusions in the alkali feldspars whereas the anhedral quartz filling the interstitial spaces between other minerals. Occasionally, it is intergrown with the potash feldspar forming graphic texture and the groundmass is stained by fine hematitic dust.



Some quartz crystals are observed enclosed poikilitically in the plagioclase and potash feldspar phenocrysts. Quartz also forms fine anhedral crystals filling the microveinlets and groundmass (Figure 3a). Plagioclase occurs in euhedral to subhedral crystals ranges from albite ( $An_5$ ) to oligoclase ( $An_{20}$ ) in composition and slightly altered to epidote, saussurite and calcite. (Figure 3b). Potash feldspars are commonly present as orthoclase or microcline occurs as elongated subhedral crystals usually characterized by shadow extinction and slightly cloudy alteration of kaolinite and sericite (Figure 3c). Some feldspar phenocrysts are enclosing inclusions of iron oxide and minute granules of quartz.

The essential minerals of the trachyandesites are plagioclase hornblende, biotite and pyroxene. Plagioclase occurs as phenocrysts as well as smaller crystals of groundmass which reach in dimensions down to microlites recognizable under the microscope. Phenocrysts of plagioclase usually show euhedral to subhedral forms (Figure 3d). However, some crystals possess subrounded form suggesting that some resorption may have occurred. The groundmass show different degrees of flow alignment giving rise to trachytic texture (Figure 3e).

In few cases, some plagioclase phenocrysts are grown together in aggregates scattered throughout the irregular fractures cutting across the twinning planes. The plagioclase phenocrysts are highly altered where lamellar twinning and

crystal outlines are obliterated (Figure 3f). It is worthy to mention that although the plagioclase feldspars occur in more than one generation, the phenocrysts and those of the groundmass is so between them.

### Analytical Techniques

Major and trace element analyses of 17 petrographically selected samples were determined by inductively coupled plasma atomic emission spectroscopy (ICP-AES) technique at the Central Laboratory in Nuclear Materials Authority (NMA), Egypt. Chemical data of the analyzed rhyolites and trachyandesites samples are shown in Tables 1 and 2. Loss on ignition (LOI) was determined by heating powdered samples for about 1h at 1000°C. Analytical precision based on duplicate analyses are expressed in terms of relative percentages and are found to vary from  $\pm 0.22$  to  $\pm 1.65\%$  for major elements and from  $\pm 4$  to  $\pm 9\%$  for trace elements.

### Geochemical Characteristics

#### 1. Geochemistry of major oxides and trace elements

Generally, rhyolites are characterized by high values of  $\text{SiO}_2$ , Cu, Y, Ba, Zr, Pb, Rb, Ga and low values of CaO,  $\text{TiO}_2$ , Zn, Sr, V, Nb when compared with trachyandesites. The highest values of  $\text{Fe}_2\text{O}_3$ , FeO, MgO,  $\text{TiO}_2$ , CaO, Cr, Ni, Zn, Sr, V and Nb contents among the trachyandesites may be attributed to a greater depth of origin from a relatively Mg-rich magma.

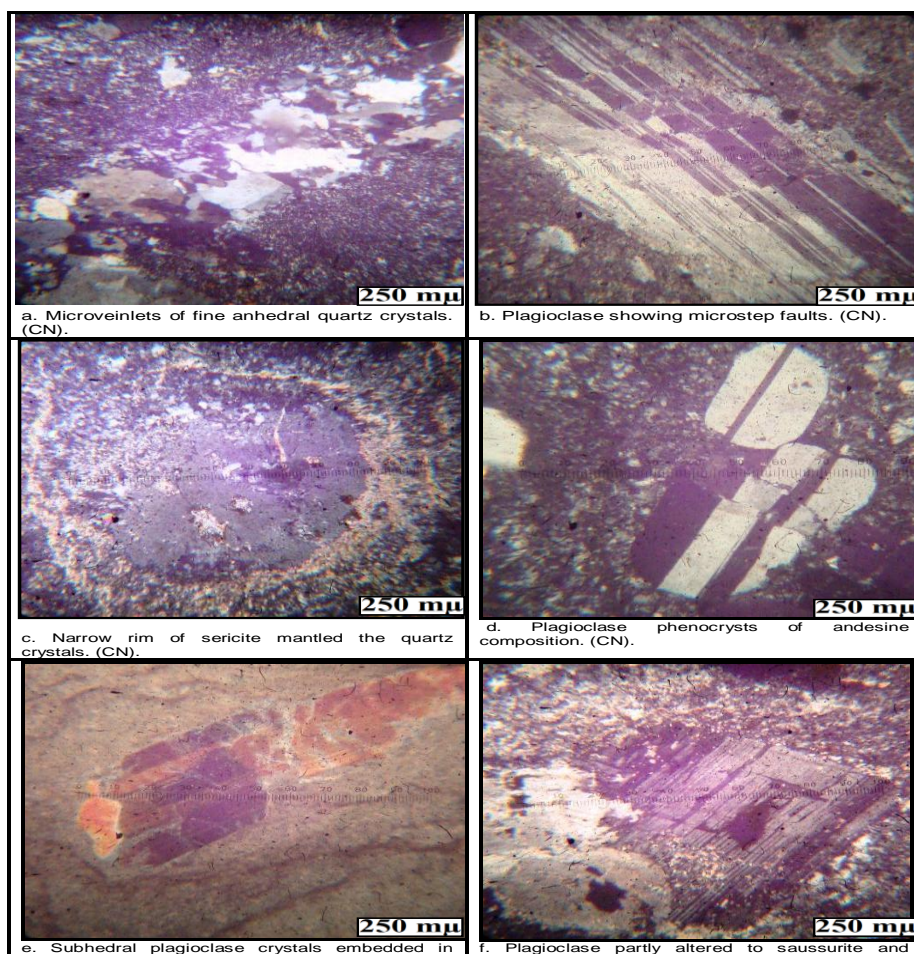


**Figure 3 (a-f).** Photomicrograph showing petrographic features

In the acidic rhyolite suite, fractional crystallization of plagioclase caused progressive depletion in CaO and Sr with increasing silica content. Also, the decrease of  $\text{Fe}_2\text{O}_3$ , FeO, MgO and somewhat Cr content with increasing silica content may imply fractionation of clinopyroxene.

Overall, trachyandesites are characterized by rather high contents and limit range of  $\text{Al}_2\text{O}_3$  (15.89–16.54 wt.%),  $\text{TiO}_2$  (1.09–1.16 wt.%),  $\text{Na}_2\text{O}$  (4.48–4.95%),  $\text{K}_2\text{O}$  (3.21–3.29),  $\text{CaO}$  (5.04–5.19 wt.%),  $\text{Fe}_2\text{O}_3$  (3.22–3.97%),  $\text{FeO}$  (3.04–3.66%),  $\text{MgO}$  (2.45–2.97%),  $\text{Rb}$  (111–119 ppm),  $\text{Zn}$  (160–167 ppm),  $\text{V}$  (163–168 ppm),  $\text{Ba}$  (301–322 ppm),  $\text{Sr}$  (303–323 ppm),  $\text{Zr}$  (145–308 ppm), and  $\text{Nb}$  (249–257 ppm).

The rhyolite volcanics (71.08–74%  $\text{SiO}_2$ ) are marked by relatively high  $\text{Al}_2\text{O}_3$  (12.04–14.01%),  $\text{Na}_2\text{O}$  (4.03–4.50%),  $\text{K}_2\text{O}$  (3.01–3.90%),  $\text{Zr}$  (353–475 ppm),  $\text{Rb}$  (116–160 ppm),  $\text{Ba}$  (215–289 ppm),  $\text{Y}$  (135–219 ppm),  $\text{Zn}$  (33–83 ppm) and  $\text{Nb}$  (67–121 ppm) and low  $\text{P}_2\text{O}_5$  (0.01–0.25%),  $\text{MgO}$  (0.09–1.12%),  $\text{CaO}$  (0.69–2.33%),  $\text{Ni}$  (7–17 ppm),  $\text{Cu}$  (10–18 ppm),  $\text{Cr}$  (18–35 ppm),  $\text{V}$  (3–7 ppm) and  $\text{Sr}$  (15–24 ppm).

Plotting of the major and trace elements versus silica content (Figures. 4, 5, 6 and 7), confirms the subdivision of the studied Dokhan Volcanics into two separate suites, separated by a large compositional gap in silica content. Moreover, Harker variation diagrams (Figures. 4, 5, 6 and 7), shows gradual decrease in  $\text{TiO}_2$ ,  $\text{Al}_2\text{O}_3$ ,  $\text{Fe}_2\text{O}_3$ ,  $\text{FeO}$ ,  $\text{MgO}$ ,  $\text{CaO}$ ,  $\text{Na}_2\text{O}$ ,  $\text{P}_2\text{O}_5$ ,  $\text{Zn}$ ,  $\text{Ba}$ ,  $\text{Cr}$ ,  $\text{Nb}$  and regular increase in  $\text{Zr}$ ,  $\text{Rb}$ ,  $\text{Ga}$ ,  $\text{Y}$ ,  $\text{Cu}$ ,  $\text{Pb}$  and somewhat  $\text{K}_2\text{O}$  with progressive increase in  $\text{SiO}_2$  content in both rhyolite and trachyandesite suites.  $\text{V}$ ,  $\text{Ni}$  and  $\text{Sr}$  elements show no apparent trend.

Based on the geochemical data given in Tables (1 and 2), a number of discrimination and correlation diagrams used to identify the chemical classification, nature of the magma and tectonic setting as well as the petrogenetic evolution of the studied Dokhan Volcanics.

## 2. Chemical Classifications

The petrographical classification of the studied Dokhan Volcanics was chemically confirmed by plotting the analytical data on the  $\text{Na}_2\text{O}+\text{K}_2\text{O}$  versus  $\text{SiO}_2$  diagram. Geochemical classification of volcanic rocks using total alkali versus silica (TAS) diagram (Cox *et al.*, 1979) shows that these volcanics are plot in the fields of rhyolite and trachyandesite (Figure 8a).

According to the  $\text{SiO}_2$  versus  $\text{Na}_2\text{O}+\text{K}_2\text{O}$  diagram recommended by the International Union of Geological Sciences (IUGS) for the classification of volcanic rocks (Le Bas *et al.* (1986) in Le Maitre, 1989) shows that the studied volcanics are rhyolite to dacite and basaltic trachyandesite (Fig.8b). The rhyolite volcanics plot in the subalkaline field and trachyandesite volcanic samples plot mostly within the alkaline field of Irvine and Barager (1971). Moreover, plotting the samples on the field for Dokhan volcanics (DV) proposed by Eliwa *et al.* (2006) indicates that most of the studied samples fall in the field of Dokhan volcanics (Figure 8b).

The  $\text{SiO}_2$  versus  $\text{K}_2\text{O}$  diagram (Figure 8c) of Boillot (1981) shows the fields of classification of volcanic rocks. The Dokhan Volcanics are distinctly low-K andesites and rhyolites. The rhyolites are medium- to high-K and cover a wide range of  $\text{K}_2\text{O}$  (Condie (1982; Figure 8c).

Based on the ( $\text{Na}_2\text{O}+\text{K}_2\text{O}$ ) and  $\text{SiO}_2$  contents Middlemost (1985) classified the volcanic rocks (Figure 8d). The plots of the investigated volcanics on this classification revealed that, the rhyolite Dokhan Volcanics as rhyolite, rhyolite dacite and alkali rhyolite. The analyzed samples of the trachyandesite fall in the fields of trachyandesite basalt and trachyandesite (Figure 8d). The investigated volcanic rocks have a wide range of  $\text{Na}_2\text{O}+\text{K}_2\text{O}$  (7.75 average of rhyolites and 7.94 average of trachyandesites) ranging from low, medium to high alkali members.

Table 1. Major oxides and trace elements of the rhyolites in Wadi Zareib.

Rock types	Rhyolites									
Oxides	1Z	2Z	3Z	4Z	5Z	7Z	10Z	15Z	16Z	17Z
$\text{SiO}_2$	73.40	72.39	74	71.08	72.20	74	72.33	73.30	71.55	72.11
$\text{TiO}_2$	0.10	0.50	0.14	0.30	0.51	0.10	0.61	0.11	0.60	0.18
$\text{Al}_2\text{O}_3$	13.40	13.71	13.50	14.01	13.21	13.40	12.98	13.60	12.04	12.8
$\text{Fe}_2\text{O}_3$	1.20	3.27	1.30	1.04	1.16	1.60	2.95	2.10	2.13	0.30
$\text{FeO}$	0.98	0.97	0.87	3.37	3.78	0.98	1.16	1.04	2.03	1.78
$\text{MgO}$	0.40	0.28	0.50	0.85	1.12	0.30	0.96	0.60	0.09	0.65
$\text{CaO}$	1.20	0.69	0.90	2.33	2.30	0.80	1.23	0.90	1.69	1.45
$\text{Na}_2\text{O}$	4.50	4.03	4.40	4.19	4.23	4.30	4.29	4.30	4.16	4.40
$\text{K}_2\text{O}$	3.90	3.08	3.50	3.69	3.68	3.70	3.20	3.80	3.01	3.10
$\text{P}_2\text{O}_5$	0.04	0.09	0.03	0.01	0.02	0.03	0.21	0.02	0.25	0.10
LOI	1.72	1.09	1.60	2.10	0.61	1.75	0.15	1.22	0.24	1.30
Total	99.9	99.9	99.9	99.3	99.6	100	99.07	99.9	99.80	99.18
	Trace elements (ppm)									
$\text{Cr}$	22	18	32	23	21	18	19	26	26	35
$\text{Ni}$	12	8	15	11	12	7	16	7	17	13
$\text{Cu}$	13	10	16	12	13	12	18	16	11	18

Table 1. Continuation

Zn	70	49	33	72	75	45	79	39	68	83
Zr	430	475	353	403	420	433	425	366	421	376
Rb	158	145	144	149	152	116	160	144	154	130
Y	205	214	175	214	218	205	214	135	219	184
Ba	289	280	256	278	284	263	215	253	277	284
Pb	56	45	43	54	56	30	54	52	55	54
Sr	16	15	17	17	18	17	16	22	24	16
Ga	49	44	44	48	46	32	45	32	44	44
V	5	4	3	5	6	4	7	4	6	5
Nb	79	71	71	75	74	79	121	67	77	75

Table 2. Major oxides and trace elements of the trachyandesites in Wadi Zareib

Rock types	Trachyandesites							Averages	
	6Z	8Z	9Z	11Z	12Z	13Z	14Z	R	T
Oxides									
SiO <sub>2</sub>	56.64	58.24	57.04	56.24	58.20	58.22	57.20	72.64	57.40
TiO <sub>2</sub>	1.13	1.11	1.12	1.16	1.09	1.12	1.10	0.32	1.12
Al <sub>2</sub> O <sub>2</sub>	16.02	16.33	15.89	16.08	16.49	16.54	16.12	13.27	16.21
Fe <sub>2</sub> O <sub>3</sub>	3.97	3.90	3.91	3.97	3.22	3.35	3.91	1.71	3.75
FeO	3.44	3.45	3.21	3.66	3.11	3.04	3.32	1.70	3.32
MgO	2.77	2.65	2.96	2.45	2.64	2.69	2.97	0.58	2.73
CaO	5.14	5.13	5.17	5.12	5.19	5.04	5.13	1.35	5.15
Na <sub>2</sub> O	4.65	4.60	4.78	4.95	4.49	4.48	4.90	4.28	4.70
K <sub>2</sub> O	3.21	3.23	3.22	3.27	3.29	3.24	3.22	3.47	3.24
P <sub>2</sub> O <sub>5</sub>	0.43	0.42	0.42	0.43	0.30	0.33	0.42	0.08	0.40
LOI	0.41	0.41	0.41	0.41	0.21	0.21	0.41	1.18	0.35
<b>Total</b>	<b>99.33</b>	<b>99.33</b>	<b>99.33</b>	<b>99.33</b>	<b>98.20</b>	<b>98.20</b>	<b>99.33</b>	--	--
	Trace elements (ppm)								
Cr	45	39	41	44	39	39	40	24	41
Ni	81	82	83	86	84	81	89	11.8	83.7
Cu	8	9	7	9	8	7	8	13.9	8
Zn	160	160	161	161	167	165	164	61.3	162.6
Zr	85	89	87	85	90	89	85	410.2	87.2
Rb	111	119	116	116	118	118	119	145.2	116.7
Y	57	58	54	57	59	59	57	198.3	57.3
Ba	322	308	322	321	301	321	322	267.9	316.7
Pb	18	19	18	17	18	18	19	49.9	18.1
Sr	303	309	308	307	307	323	303	17.8	308.6
Ga	22	24	25	29	25	26	24	42.8	25
V	166	164	167	165	166	163	168	4.9	165.6
Nb	257	255	254	251	254	255	249	78.9	253.6

R. The averages chemical composition of the studied rhyolites.

T. The averages chemical composition of the studied trachyandesites.

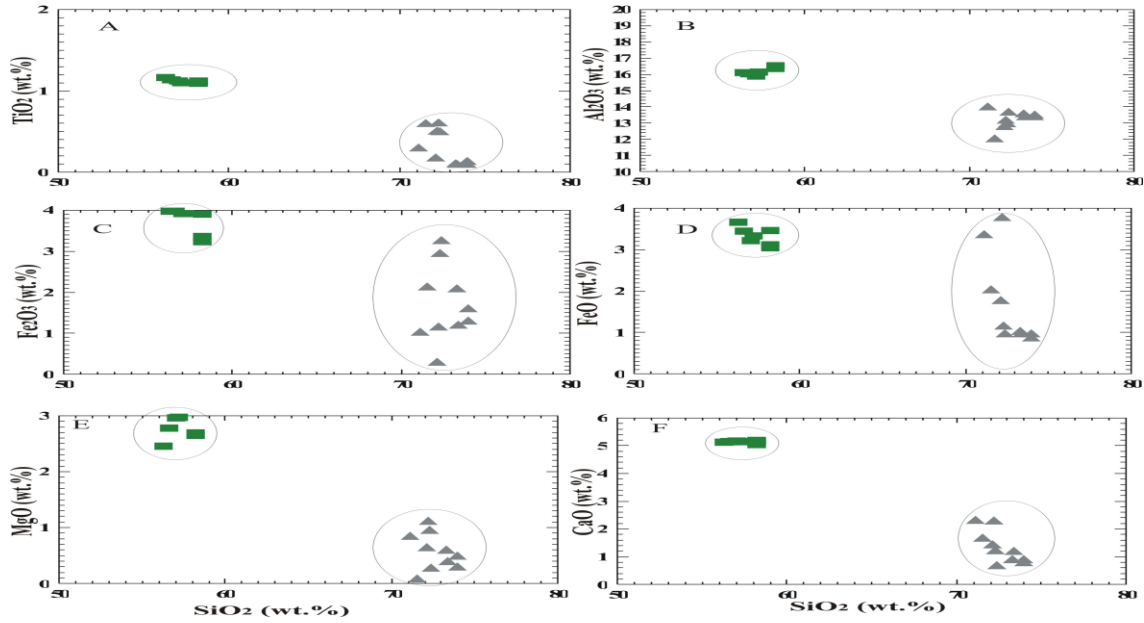


Figure 4. Variations of major oxides against SiO<sub>2</sub> (wt.%) for the studied Wadi Zareib Dokhan Volcanics. Symbols as in Figure 8a

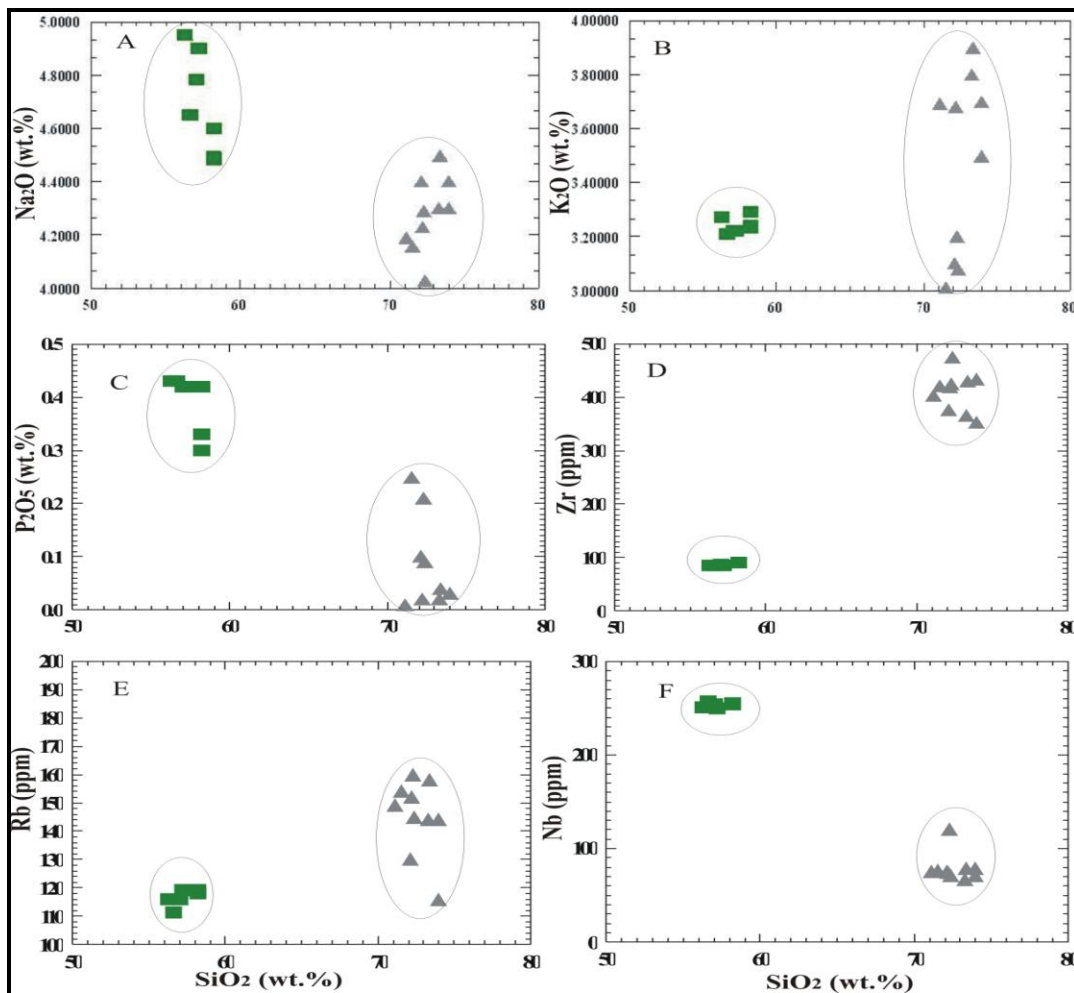


Figure 5. Variations of some major oxides and trace elements (ppm) against SiO<sub>2</sub> (wt.%) for the studied Wadi Zareib Dokhan Volcanics. Symbols as in Figure 8a.



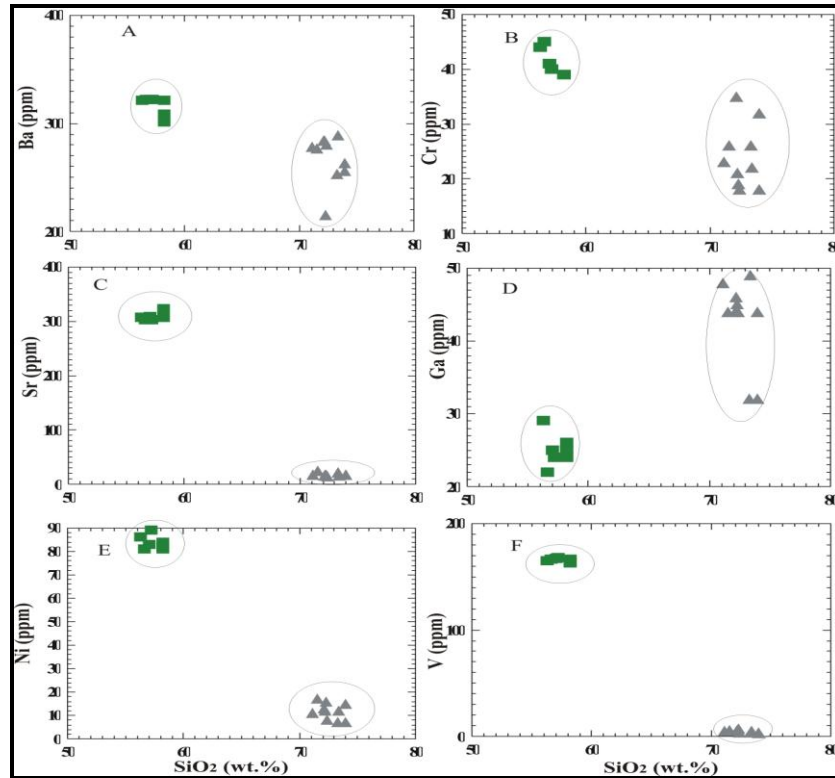


Figure 6. Variation diagrams of trace elements (ppm) against SiO<sub>2</sub> (wt.%) for the Wadi Zareib Dokhan Volcanics. Symbols as in Figure 8a.

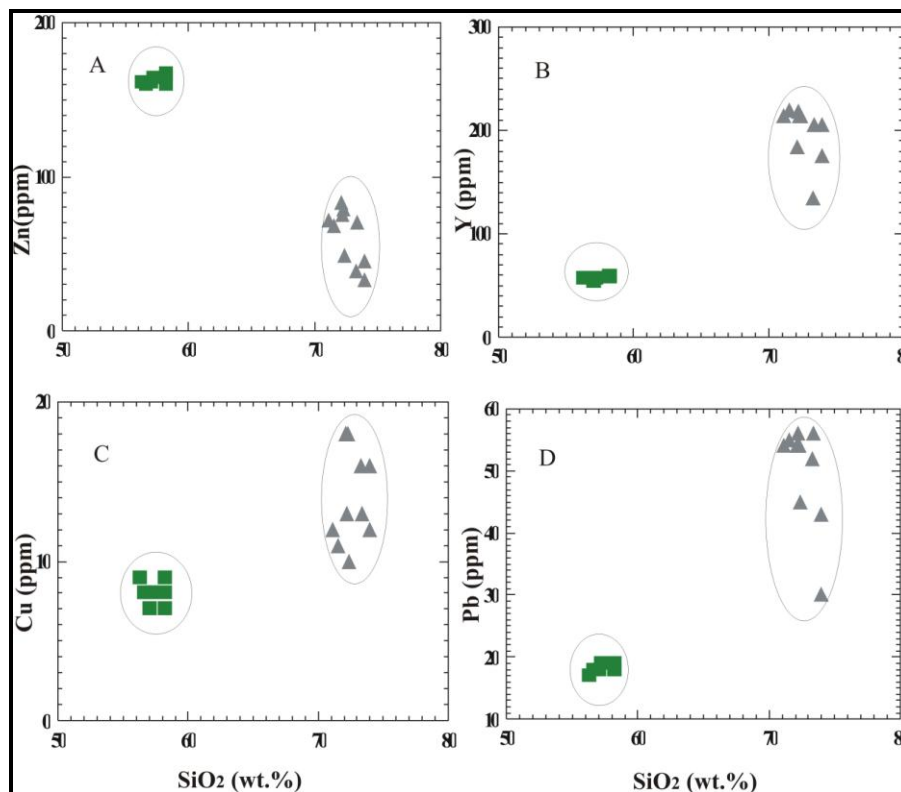


Figure 7. Variation diagrams of trace elements (ppm) against SiO<sub>2</sub> (wt. %) for the Wadi Zareib Dokhan Volcanics. Symbols as in Figure 8a

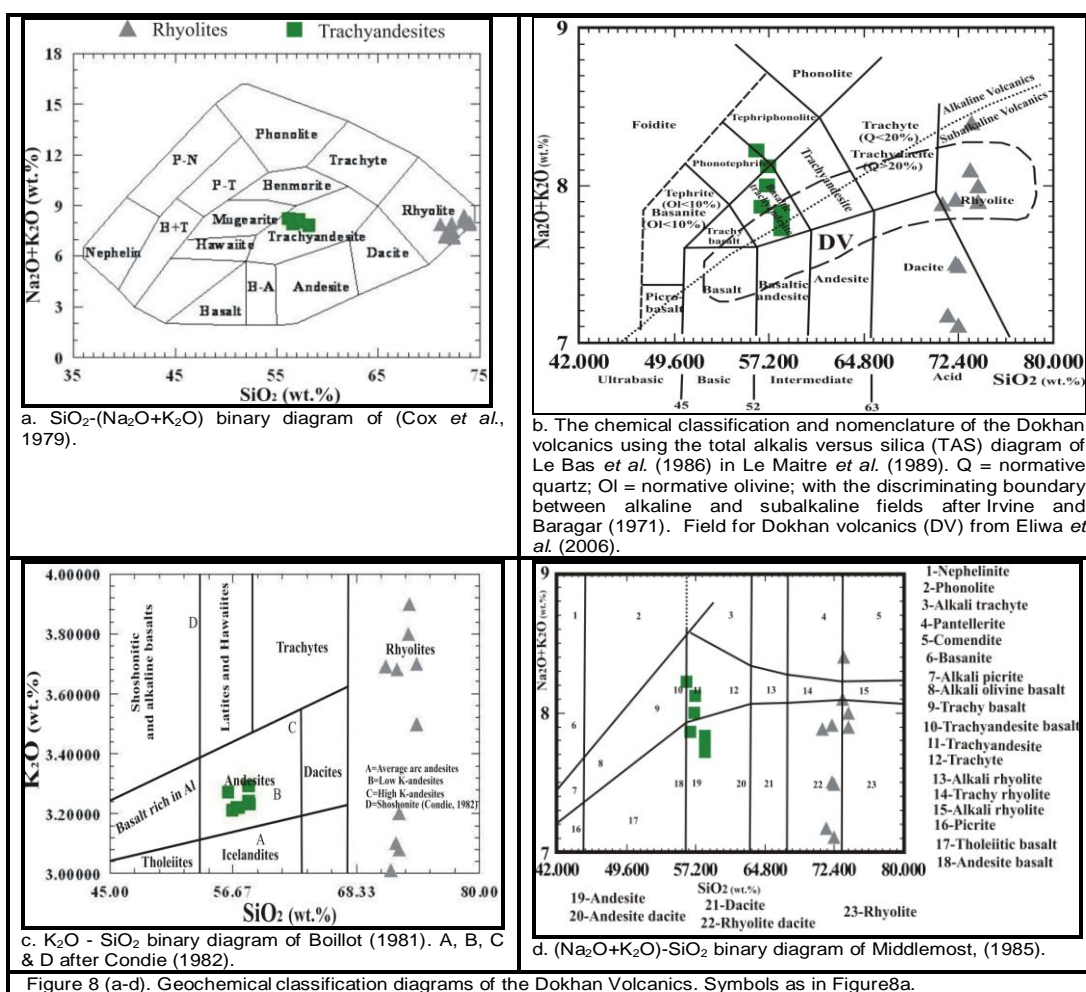
### 3. Source and Fractionation

Rhyolites have generally been attributed to crustal melting (Tronnes, 2002). Meganck (2004), argued against partial melting for rhyolites and dacites based primarily on Zr concentrations.

Most major and trace element variation diagrams of Tronnes (2002) and Meganck (2004) show trends for the trachyandesites that are generally compatible with a model of crystal fractionation in a shallow magma chamber. The concentrations of MgO, FeO, and CaO decrease with increasing SiO<sub>2</sub> content, compatible with crystal fractionation of plagioclase and clinopyroxene. When plotted against MgO, the concentrations of FeO, TiO<sub>2</sub>, and P<sub>2</sub>O<sub>5</sub> initially increase and then decrease, indicating the fractionation of Fe-Ti oxides and apatite followed the peak.

Several variation diagrams, such as those in Figure 9, show additional trends that cannot be completely explained by crystal fractionation. Rhyolites plot on a trend of decreasing Zr with increasing SiO<sub>2</sub>, which, combined with thin-section observations, indicates late zircon fractionation. As seen in Figure 9d, the concentration of Zr is lower in the more evolved trachyandesites than in the rhyolites.

Although most of the trachyandesites seem to follow a trend of fractional crystallization (Figure 9 b and c), the rhyolites require a more complex explanation involving both fractional crystallization and magma mixing.



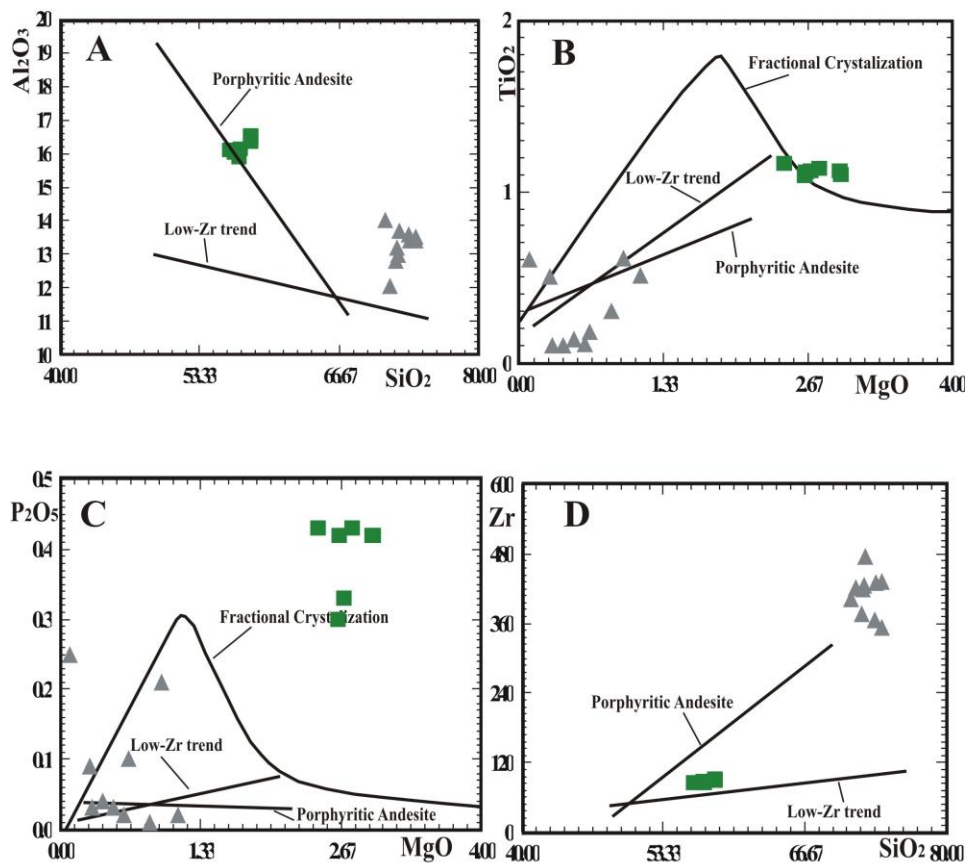


Figure 9 (a-d). Variation diagrams showing various trends (After, Tronnes, 2002 and Meganck, 2004). These trends support crustal fractionation and magma mixing. Symbols as in Figure 8a

#### 4. Adakitic affinity

As originally defined (Defant and Drummond, 1990; Maury *et al.*, 1996; Martin, 1999), adakites form suites of intermediate to felsic rocks whose compositions range from hornblende–andesite to dacite and rhyolite; basaltic members are lacking. In these lavas, phenocrysts are mainly zoned plagioclase, hornblende, and biotite; orthopyroxene and clinopyroxene phenocrysts are known only in mafic andesites from the Aleutians and Mexico (Kay, 1978; Rogers *et al.*, 1985; Calmus *et al.*, 2003). Accessory phases are apatite, zircon, sphene and titanomagnetite. The rocks have  $\text{SiO}_2 > 56$  wt.%, high  $\text{Na}_2\text{O}$  contents ( $3.5 \text{ wt.}\% \leq \text{Na}_2\text{O} \leq 7.5 \text{ wt.}\%$ ) and correlated low  $\text{K}_2\text{O}/\text{Na}_2\text{O}$  ( $\sim 0.42$ ). Their  $\text{Fe}_2\text{O}_3 + \text{MgO} + \text{MnO} + \text{TiO}_2$  contents are moderately high ( $\sim 7$  wt.%), with high Mg# ( $\sim 0.51$ ) and high Ni and Cr contents (24 and 36 ppm, respectively). Defant and Drummond (1990) also reported typically high Sr contents ( $> 400$  ppm), with extreme concentrations reaching 3000 ppm. Rare earth element (REE) patterns are strongly fractionated  $(\text{La}/\text{Yb})_{\text{N}} > 10$  with typically low heavy REE (HREE) contents ( $\text{Yb} \leq 1.8$  ppm,  $\text{Y} \leq 18$  ppm). Amongst the defining geochemical characteristics of adakites are their HREE, Y and Sr contents, and two widely used discriminant diagrams are  $(\text{La}/\text{Yb})_{\text{N}}$  versus  $\text{Yb}_{\text{N}}$  (Martin, 1987 and 1999) (where N indicates chondrite normalization), and  $\text{Sr}/\text{Y}$  versus Y (Defant and Drummond, 1990).

As proposed by Defant and Drummond (1990 and 1993), certain geochemical characteristics can be used to discriminate between normal calc-alkaline lavas and adakites. On these bases, trachyandesite Dokhan lavas are adakite of delaminated lower crust-derived adakitic rocks and rhyolites are normal calc-alkaline lavas (arc magmatic rocks) of thick lower crust-derived adakitic rocks (Figure 10a-c). The lavas in the Dokhan Volcanics are belonging to both the low-silica adakite (LSA) and high-silica adakite (HSA) groups. Martin and Moyen (2003) and Martin *et al.* (2005) identified two distinct adakite groups: high- $\text{SiO}_2$  adakites (Rhyolites, HSA;  $\text{SiO}_2 > 60$  wt.%) and low- $\text{SiO}_2$  adakites (Trachyandesites, LSA;  $\text{SiO}_2 < 60$  wt.%; Figure 11a-e).

It is generally believed that reaction between pure slab melts and surrounding peridotite in the sub-arc mantle wedge results in the high Mg-number and MgO contents typical of adakites (Figure 10c). In the Figure 10c, the Wadi Zareib samples fall within the fields of “thick lower crust-derived adakite rock” and “delaminated lower crust-derived adakitic rocks”.

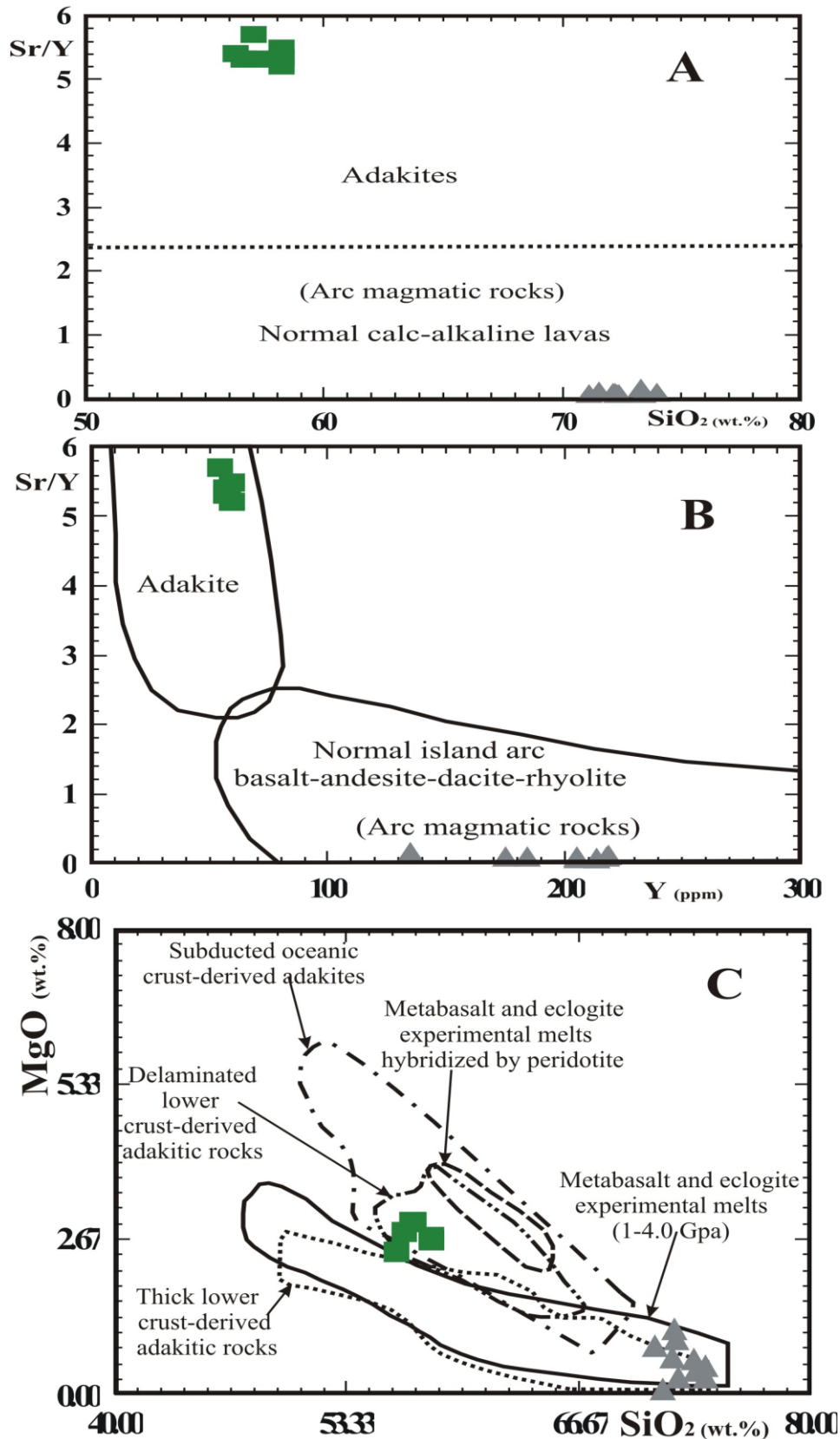


**Figure 10.** Binary relations can be used to discriminate between normal calc-alkaline lavas and adakites: (A) SiO<sub>2</sub> versus Sr/Y and (B) Y versus Sr/Y after Defant and Drummond (1990 and 1993) and (C) MgO versus SiO<sub>2</sub>.

The field of metabasalt and eclogite experimental melts (1–4.0 GPa) is from Rapp *et al.* (1991, 1999, 2002), Sen and Dunn (1994), Rapp and Watson (1995), Prouteau *et al.* (1999), Skjerlie and Patiño Douce (2002) and references therein. The field of metabasalt and eclogite experimental melts hybridized with peridotite is after Rapp *et al.* (1999). The field of subducted oceanic crust-derived adakites is constructed using data from Defant and Drummond (1990), Kay and Mahlburg-Kay (1993), Drummond *et al.* (1996), Stern and Kilian (1996), Sajona *et al.* (2000), Aguillón-Robles *et al.* (2001), Defant *et al.* (2002), Calmus *et al.* (2003), Martin *et al.* (2005) and references therein. Data for thick lower crust-derived adakitic rocks are from Atherton and Petford (1993), Muir *et al.* (1995), Petford and Atherton (1996), Johnson *et al.* (1997), Xiong *et al.* (2003). Symbols as in Figure 8a.

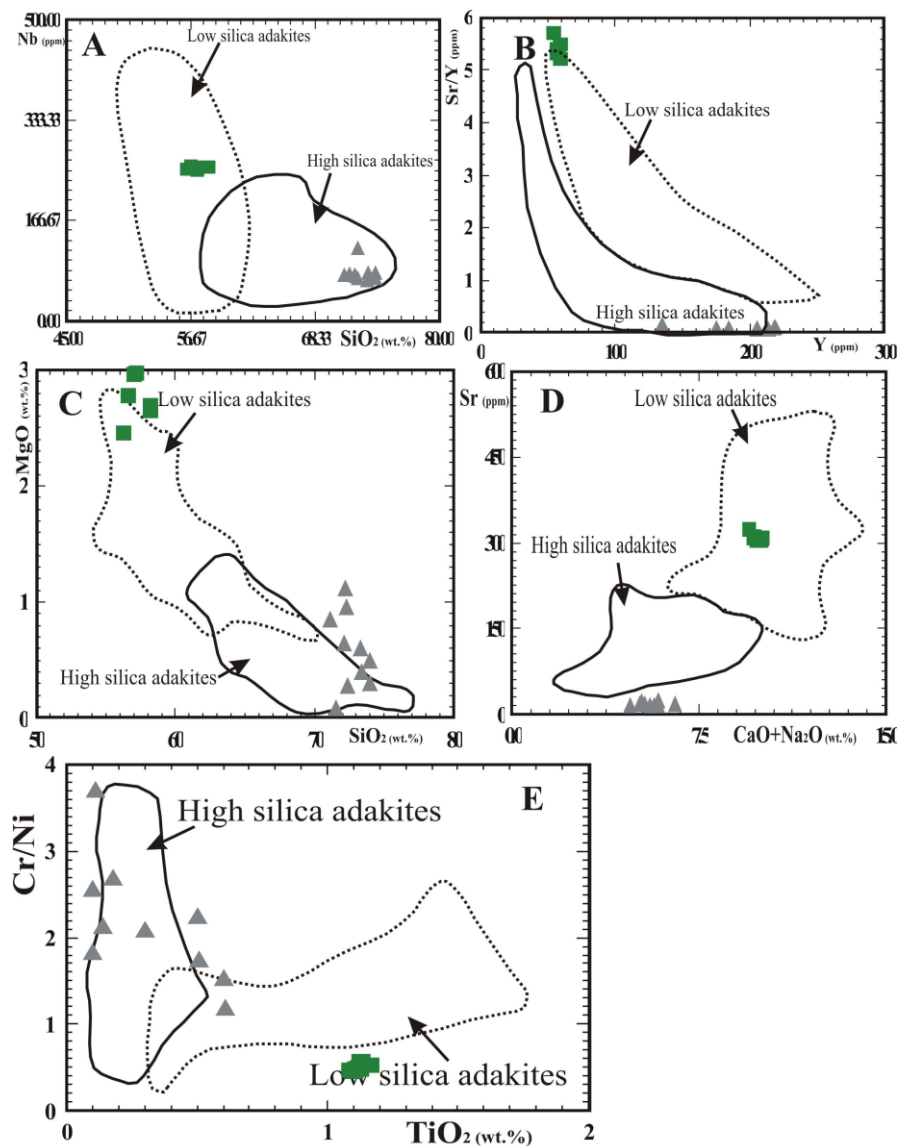
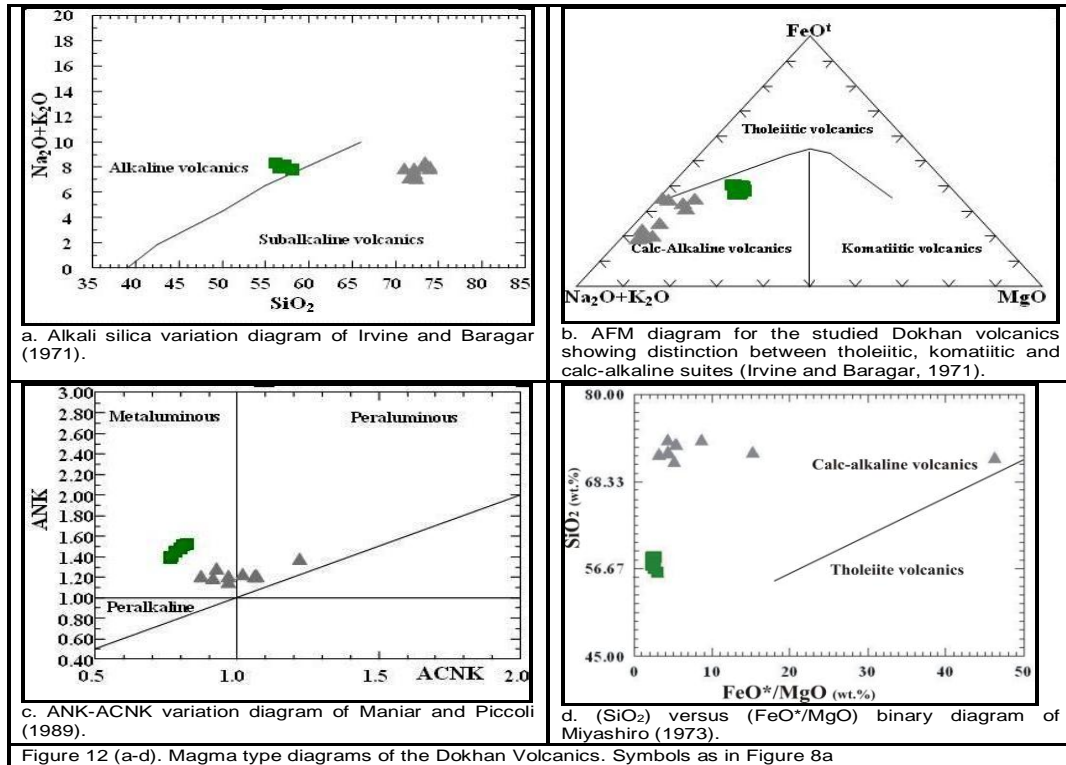


Figure 11. (A) Nb versus  $\text{SiO}_2$ ; (B)  $\text{Sr}/\text{Y}$  versus  $\text{Y}$ ; (C)  $\text{MgO}$  versus  $\text{SiO}_2$ ; (D)  $\text{Sr}$  versus  $(\text{CaO}+\text{Na}_2\text{O})$  and (E)  $\text{Cr}/\text{Ni}$  versus  $\text{TiO}_2$  diagrams comparing high- $\text{SiO}_2$  adakites (HSA) and low- $\text{SiO}_2$  adakites (LSA) of Martin and Moyen (2003) and Martin *et al.* (2005). Symbols as in Figure 8a

## 5. Nature of the Magma

On the Alkali silica variation diagram proposed by Irvine and Baragar (1971), the data points of the studied rhyolite samples fall in the field of subalkaline volcanics. The trachyandesite samples plotted in the field of alkaline volcanics due to the low content of  $\text{SiO}_2$  (Figure 12a). The studied Dokhan Volcanic samples are plotted on the AFM diagram of Irvine and Baragar (1971). They exhibit calc-alkaline affinity (Figure 12b).

The  $\text{Al}_2\text{O}_3/(\text{Na}_2\text{O}+\text{K}_2\text{O})$  versus  $\text{Al}_2\text{O}_3/(\text{CaO}+\text{Na}_2\text{O}+\text{K}_2\text{O})$  diagram of Maniar and Piccoli (1989) shows that all the studied trachyandesite samples and some rhyolite samples are metaluminous except three samples of rhyolite exhibit peraluminous nature (Figure 12c). The relationship between  $\text{SiO}_2$  and  $\text{FeO}^*/\text{MgO}$  ratio of Miyashiro (1973) is used to differentiate between the calc-alkaline and tholeiitic. The plots of the investigated volcanics on this diagram indicate that, these Dokhan Volcanics are of calc-alkaline affinity (Figure 12d).



## 6. Tectonic Setting

The petrographic and geochemical data revealed the alkaline affinity of the studied trachyandesites, whereas the rhyolites show a subalkaline character. The geochemical signatures of igneous suites often suggest tectonic setting prevailing at the time of emplacement.

The tectonic setting of the Dokhan Volcanics is considered as one of the matters of controversy. The geochemical studies indicate that they are calc-alkaline orogenic complex of island arc with continental type crust (Basta *et al.*, 1980; Gas, 1982; Heikal and Ahmed, 1984) or Andean type continental margins (El-Gaby *et al.*, 1988 and 1990). There are three various models are proposed for the emplacement of the Dokhan Volcanics.

The first is proposed by Stern *et al.* (1984 and 1988); Stern and Hedge (1985); Stern and Gottfried (1986) and El-Desoky (2013), in which they related to the Dokhan Volcanics eruptions to a period of strong extension (or orogenic) analogous to that of the Oslo rift. They regarded the Dokhan volcanics and the younger granite as bimodal igneous activity characteristic of rifting. They also stated that the temporal and spatial emplacement of mantle-derived bimodal dyke and Dokhan volcanics swarms in eastern Egypt marks the transition in the tectonic style from compressional to strong north/south- to northwest/southeast-directed crustal extension at approximately 600 Ma.

The second model stated by Rosseter and Monrad (1983), in which the Dokhan Volcanics were interpreted to have been formed in a transitional environment between compressive and extensional tectonic settings. This is based mainly on: (I) age relation where they postdate the calc-alkaline subduction-related rocks and are of similar age to the postorogenic younger granitoids; (II) the similarity of the chemical composition of these volcanics to those seen in orogenic belts but with high Zr, Nb, Ti, and alkalis.

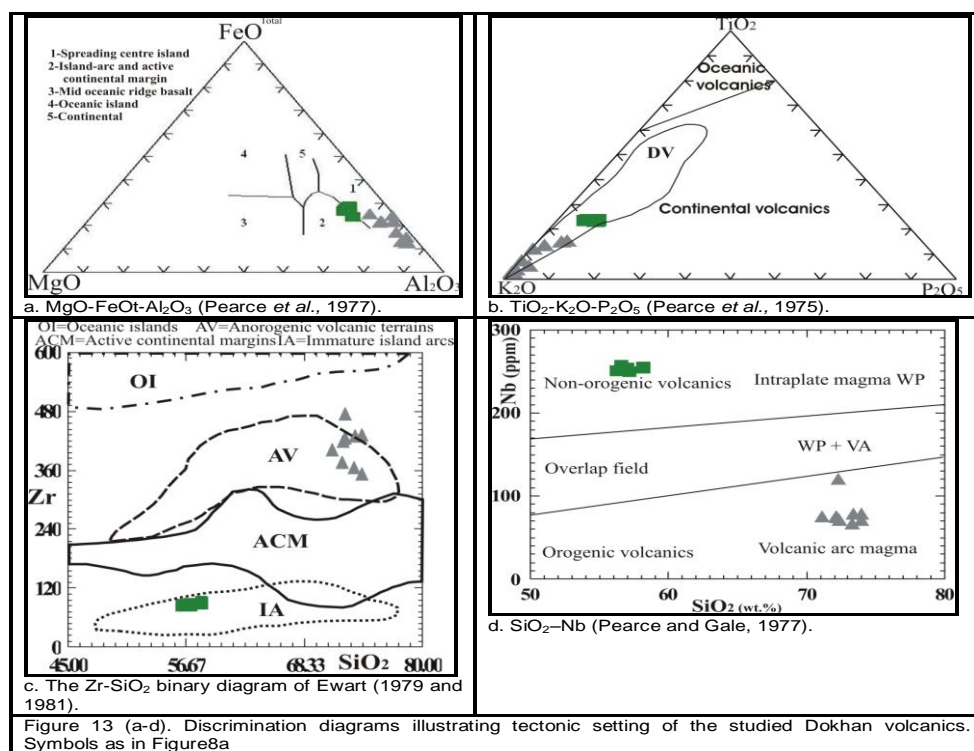
The third model is proposed by Basta *et al.* (1980), Ragab (1987), El Gaby *et al.* (1989) and Abdel Rahman (1996), where he referred the Dokhan Volcanics to a subduction-related environment (compressional tectonic settings). Based on the geochemical characteristics, they show that the Dokhan volcanics are calc-alkaline in nature and their trace element and REE contents resemble those of arc related orogenic suites and thus they were erupted during the final stages of active subduction beneath the Eastern Desert of Egypt. However, the younger granite intrusions in Eastern

Egypt are massive and undeformed post orogenic granitoids with typical A-type characteristics (Stern and Gottfried, 1986; Sylvester, 1989; Hassanen, 1997; Moghazi, 1999; Mohamed *et al.*, 1999).

The study Dokhan Volcanics are plotted on tectonic discrimination diagrams (Figure 13), which are based on virtually immobile elements (Zr, TiO<sub>2</sub> and Nb). The tectonomagmatic position of the studied Dokhan Volcanics can be assigned using some discrimination diagrams based on both major and trace elements. On the FeO<sup>\*</sup>-MgO-Al<sub>2</sub>O<sub>3</sub> discrimination diagram (Figure 13a) of Pearce *et al.* (1977) indicate that the rhyolites are plotted close to spreading Centre Island field due to the enrichment in Al<sub>2</sub>O<sub>3</sub> content. The trachyandesite samples fall on the line separations spreading Centre Island and island arc and active continental margin fields. A ternary K<sub>2</sub>O-TiO<sub>2</sub>-P<sub>2</sub>O<sub>5</sub> diagram (Figure13b) of Pearce *et al.* (1975), illustrates that the investigated Dokhan Volcanics erupted in a continental rather than in oceanic setting

On the Zr- SiO<sub>2</sub> variation diagram of Ewart (1979 and 1981), the majority of the plotted rhyolite points fall within the anorogenic volcanic terrains and trachyandesite samples lie in the immature island arcs field due to low value of Zr content (Figure13c).

On the SiO<sub>2</sub> versus Nb variation diagram of Pearce and Gale (1977), the trachyandesite points are distributed in the field of non-orogenic intraplate magma (WP) and rhyolites fall in orogenic volcanic arc magma (Figure13d) due to decrease of Nb contents in these rocks. These diagrams mostly indicate that the Dokhan Volcanics erupted in an arc environment with thicker (continental) crust.



## 7. Petrogenesis

A number of tectonomagmatic discrimination diagrams have been used and the most commonly used discriminants are TiO<sub>2</sub>, K<sub>2</sub>O, P<sub>2</sub>O<sub>5</sub>, MgO, Al<sub>2</sub>O<sub>3</sub>, FeO, Zr, Nb and SiO<sub>2</sub>. It is also a common practice to compare the trace elements from known and unknown tectonic environments using spider diagrams. When plotted on an incompatible trace element diagram (often referred to as a spider diagram), calc-alkaline rocks show an irregular pattern with many peaks, unlike the relatively smooth patterns exhibited by chondrites.

Dokhan volcanics is highly likely that crystal fractionation involve assimilation of crustal materials (Stern and Gottfried, 1986). The geochemical trends of major oxides and trace elements of the rhyolites and trachyandesites may suggest their co-magmatic nature (Figure 14 and 15). These rocks were derived from a single magma and suffered subsequence fractional crystallization. The MORB-normalized spider-diagram is presented in figure (15). The patterns are characterized by high concentration of Y, Ba, Zr and Rb and depletion Ni, V, Sr, Cu and Cr.

Wilson (1989) distinguished that in active continental margin arc setting; the crust and the mantle portion of the continental lithosphere are additionally involved, making this one of the most complex magma generation environment of

the earth. The elements Y, Ba, Zr and Rb show negative anomalies (enriched) relative to elements like Ni, V, Sr, Cu and Cr (Figure 14 and 15).

Accordingly, the Dokhan Volcanics have geochemical characteristics of both subduction-related and within-plate settings. This was previously noted by many authors and has led to a debate on the convergent margin versus within-plate geotectonic setting for these volcanics.

The high mean values of the  $K_2O$  (3.47% in rhyolites and 3.24 in trachyandesites) and alkalis (7.75% in rhyolites and 7.24 in trachyandesites) indicate a secondary feature taking into account the emplacement of the Dokhan Volcanics in a sedimentary terrain, which was probably a source of alkali-rich medium during the intrusion. The narrow range of the concentrations of incompatible elements such as Zn and Ni indicates homogeneity in incompatible elements in source material.

## DISCUSSIONS

Geochemical and petrographic data are consistent with a magma mixing origin for the plagioclase-phyric trachyandesite, with mafic magma, felsic magma and plagioclase phenocrysts. Also, the phenocryst assemblage in the rhyolite indicates the likelihood of formation by partial melting of the crust.

Several studies have been carried out to reveal the petrogenesis of the Dokhan Volcanics and concluded that there was a significant role of fractional crystallization of basaltic magma coupled with minor crustal contamination controlled their magmatic evolution (Stern and Gottfried, 1986; El-Gaby *et al.*, 1989; Abdel-Rahman, 1996; Mohamed *et al.*, 2000; Saleh, 2003; Moghazi, 2003; El Sayed *et al.*, 2004; Eliwa *et al.*, 2006; El-Desoky, 2013). The present studies carried out on the geochemistry of the Wadi Zareib Dokhan Volcanics in the Egyptian Central Eastern Desert revealed that they have medium- to high-K calc-alkaline affinities.

The interpretations of tectonic setting of the Dokhan Volcanics are still vague and the controversy is centered especially around whether Dokhan volcanics have been formed in (1) a subduction-related environment (Ragab, 1987; El Gaby *et al.*, 1988 and 1990; Hassan and Hashad, 1990; Abdel Rahman, 1996; Hassan *et al.*, 2001; Saleh, 2003), (2) a rift-environment associated with extension after crustal thickening (Stern *et al.*, 1984 and 1988; Stern and Gottfried, 1986; Willis *et al.*, 1988; Stern, 1994; Fritz *et al.*, 1996; Mohamed *et al.*, 2000; El-Desoky, 2013), or (3) during transition between subduction and extension (Ressetar and Monard, 1983; Moghazi, 2003; El Sayed *et al.*, 2004; Eliwa *et al.*, 2006).

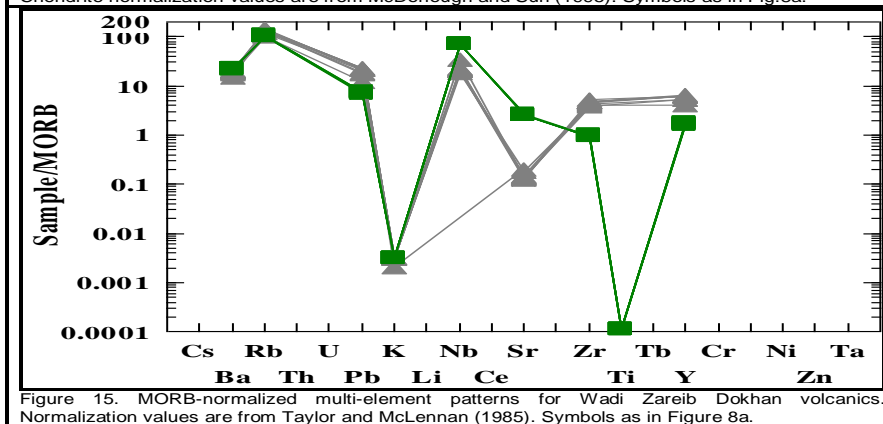
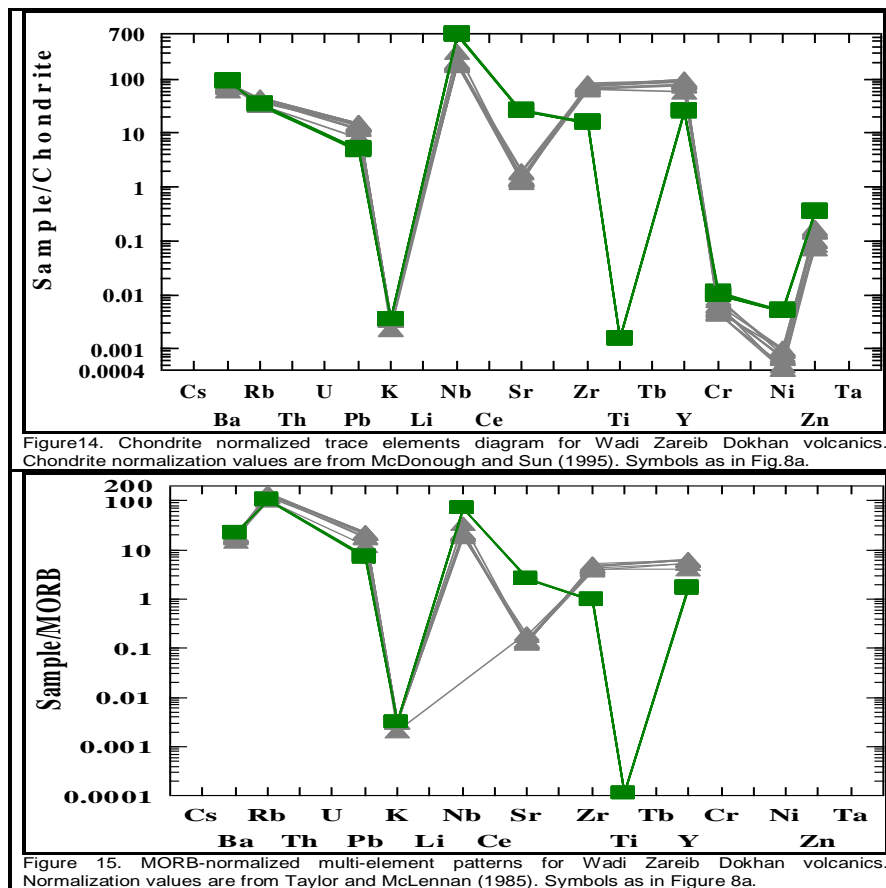
Experimental studies have demonstrated that zircon, when crystalline, has low solubility in crustal melts and fluids (Watson, 1979; Waston and Harrison, 1983; Ayers and Watson, 1991). Zirconium (Zr) commonly forms a separate phase, the mineral zircon ( $ZrSiO_4$ ). In the studied rhyolites, Zr, Ba, Rb, Y and Nb are usually incompatible and are typically concentrated in residual silicate liquids until zircon saturation occurs (Watson, 1979; Waston and Harrison, 1983).

Partial melting of the crust and magma ascent: It was argued by Gunnarsson *et al.* (1998) that rhyolites are formed by two stage partial melting of crustal material. Partial melting processes can create felsic magmas in equilibrium with olivine and pyroxene (generally uncommon in rhyolites) due to melting at high temperatures under water-poor conditions. The presence of these phenocrysts in the present samples from the rhyolite flow leads to hypothesize that they formed by this process rather than by fractional crystallization, during which hydrous ferromagnesian silicates (such as biotite and hornblende, which are not found in the flow) are typically stable.

Magma mixing: Textural and chemical characteristics of the plagioclase-phyric trachyandesite support an origin by mixing of mafic and felsic magmas. However, using the compositions of the rhyolite flow and different trachyandesite flows from my field area as hypothetical mixing end members; it does not appear possible to form the trachyandesite by simple mixing of two magmas. By including the plagioclase phenocrysts as a third independent mixing component, however, a reasonable mixing model can be calculated. Harker diagrams ( $Al_2O_3$ , CaO, and  $Na_2O$  versus  $SiO_2$ , Figure 4 and Figure 5) were used to determine possible mixing proportions of plagioclase phenocrysts, trachyandesite and rhyolite

There is a genetic relationship between high-K calc-alkaline magmatism and subduction zones (Peccerillo, 1985; Rogers and Hawkesworth, 1985). Trace element enrichments in large ion lithophile elements (LILE) and light rare earth elements (LREE) combined with relative depletions in the high field strength elements (HFSE) are common to these arc lavas (Gill, 1981; Wilson, 1989). However, the eruption of high-K magmas with a typical arc trace element signature is recorded post-dating active subduction and occurs synchronous with uplift, extension or strike-slip motion (Sloman, 1989). The interpretations of these rocks indicate that chemical heterogeneities, produced in the mantle via metasomatism, can exist for substantial periods of time after cessation of subduction (Rogers *et al.*, 1987; Thirwall, 1988; Sloman, 1989).





## CONCLUSIONS

Based on the data interpretation of the field geology, petrography, geochemistry and petrogenesis studies, the following conclusions can be investigated that the studied Dokhan Volcanics represent a calc-alkaline volcanic rocks and showing gradual transition from trachyandesitic rocks to rhyolitic rocks.

The magma reservoir is thought to have resulted from crustal melting caused by intrusion of acidic and intermediate magmas in the crust as the observed geochemical features are explained with extensive quartz + plagioclase + minor amphibole fractionation. The earliest eruptive products, build the Zareib Dokhan Volcanics and possibly also both domes and dykes from the northern parts of the Eastern Desert. At that time the chamber was probably smaller and less acidic melts (up to rhyodacites) coming from deeper parts could easily reach the surface.

Rhyolites geochemically range in composition from rhyolite to rhyodacite originated from calc-alkaline and metaluminous magma type that developed in anorogenic regime (active continental margin) but their emplacement follows the cessation of subduction in an extensional-related tectonic setting.

The present data agree with the interpretation of Stern *et al.* (1984 and 1988); Jarrar *et al.* (1993); Beyth *et al.* (1994), in which the Wadi Zareib Dokhan Volcanics represent a transitional period from compressional to extensional tectonic regime in Central Eastern Egypt where anorogenic magmatism began.

## ACKNOWLEDGEMENTS

The authors appreciate the helpful reviews and constructive comments of Prof. Mahmoud M. Hassaan, Geology Department, Faculty of Science, Al-Azhar University. The authors also are grateful to Prof. Ewais M. Moussa, Professor of Geochemistry, Head of isotope Department, Nuclear Materials Authority for providing laboratory facility for chemical analysis and fruitful discussion.

## References

- Abdel-Rahman AM(1996). Pan-African volcanism: petrology and geochemistry of the Dokhan Volcanic suite in the northern Nubian Shield. *Geol. Mag.* 133: 17–31.
- Aguillón-Robles A, Calmus T, Bellon H, Maury RC, Cotton J, Bourgois J, Michaud F(2001). Late Miocene adakites and Nben riched basalts from Vizcaino Peninsula, Mexico: indicators of East Pacific Rise subduction below southern Baja California: *Geology*, 29: 531–534.
- Ahmed AM (1983). Some petrographical and geochemical studies of Gabal Abu Had volcanics, North Eastern Desert, Egypt. M.Sc. Thesis, Al-Azhar University, Faculty of Science.
- Akaad MK (1972). A contemplation and assessment of the 1960-1961 classification of rocks of the Central Eastern Desert, *Annal. Geol. Surv. Egypt*, II, 19-45.
- Akaad MK, Abu El-Ela AM (2002). Geology of the Basement Rocks in the Eastern Half of the Belt between Latitudes 25°30' and 26°30'N, Central Eastern Desert, Egypt. *Geol. Surv.*, paper No. 78.
- Akaad MK, Noweir AM (1980). Geology and lithostratigraphy of the Arabian Desert orogenic belt of Egypt between latitudes 25°35'\_N and 26°30'\_N. *Inst. Appl. Geol. Jeddah Bull.* 3: 127–135.
- Allen PA (2007). The Huqf Supergroup of Oman: basin development and context for Neoproterozoic glaciation. *Earth Science Reviews.* 84: 139–185.
- Atherton MP, Petford N (1993). Generation of sodium-rich magmas from newly underplated basaltic crust. *Nature.* 362: 144– 146.
- Ayers JC, Watson EB (1991). Solubility of apatite, monazite, zircon and rutile in supercritical aqueous fluids with implications for subduction zone geochemistry. *Philosophical Transactions. Royal Society of London.* 335: 365–375.
- Basta EZ, Kotb H, Awadalla MF (1980). Petrochemical and geochemical characteristics of the Dokhan Formation at the type locality, Jabal Dokhan, Eastern Desert, Egypt. *Inst. Appl. Geol. Jeddah Bull.* 3: 121–140.
- Beadnell HJL (1924). Report on the geology of the Red Sea coast between Quseir and Wadi Ranga. *Petrol. Res. Bull.*, No. 13, Cairo.
- Bentor YK (1985). The crustal evolution of the Arabo-Nubian Massif with special reference to the Sinai Peninsula. *Precam. Res.* 28: 1–74.
- Beyth M, Stern RJ, Altherr R, Kröner A (1994). The late Precambrian Timna igneous complex, southern Israel: evidence for comagmatic-type sanukitoid monzodiorite and alkali granite magma. *Lithos.* 31: 103–124.
- Boillot G (1981). Geology of the continental margins. Longman London. Pp. 115.
- Brown M (2007). Metamorphic conditions in orogenic belts: a record of secular change *International Geology Review* 49:193–234.
- Calmus T, Aguillon-Robles A, Maury RC, Bellon H, Benoit M, Cotton J, Bourgois, J., Michaud, F., 2003. Spatial and temporal evolution of basalts and magnesian andesites (“bajaites”) from Baja California, Mexico: the role of slab melts. *Lithos* 66 (1–2): 77–105.
- Clark C, Collins AS, Santosh M, Taylor R, Wade BP (2009). The P–T–t architecture of a Gondwanan suture: REE, U–Pb and Ti-in-zircon thermometric constraints from the Palghat Cauvery shear system, South India. *Precambrian Research.* 174: 129–144.
- Collins AS (2006). Madagascar and the amalgamation of Central Gondwana. *Gondwana Research.* 9: 3–16.
- Collins AS, Clark C, Chetty TRK, Santosh M (2010). Ediacaran–Cambrian tectonic evolution of southern India. *Indian J. Geol.* 80: 23–40.
- Collins AS, Clark C, Sajeev K, Santosh M, Kelsey DE, Hand M (2007). Passage through India: the Mozambique Ocean suture, high pressure granulites and the Palghat–Cauvery shear system. *Terra Nova.* 19: 141–147.
- Collins AS, Kröner A, Fitzsimons ICW, Razakamanana T(2003). Detrital footprint of the Mozambique Ocean: U/Pb SHRIMP and Pb evaporation zircon geochronology of metasedimentary gneisses in eastern Madagascar. *Tectonophysics.* 375: 77–99.
- Collins AS, Pisarevsky SA (2005). Amalgamating eastern Gondwana: the evolution of the Circum-Indian Orogens. *Earth Science Reviews.* 71: 229–270.
- Collins AS, Windley BF (2002). The tectonic evolution of central and northern Madagascar and its place in the final assembly of Gondwana. *J. Geol.* 110: 325–340.
- Condie KC (1982). Plate tectonic model for Proterozoic continental accretion in the southwest United States: *Geology.* 10: 37-42.
- Cox KG, Bell JD, Pankhurst RJ (1979). The interpretation of igneous rocks. London. Allen and Unwine. Pp. 450.
- Dalziel IWD (1997). Neoproterozoic–Paleozoic geography and tectonics: review, hypothesis, environmental speculation. *Geological Society of America Bulletin.* 109: 16–42.
- Defant MJ, Drummond MS (1990). Derivation of some modern arc magmas by melting of young subducted lithosphere. *Nature.* 347: 662–665.
- Defant MJ, Drummond MS (1993). Mount St. Helens: potential example of the partial melting of the subducted lithosphere in a volcanic arc. *Geology.* 21: 547–550.
- Defant MJ, Xu JF, Kepezhinskas P, Wang Q, Zhang Q, Xiao L(2002). Adakites: some variations on a theme: *Acta Petrologica Sinica.* 18: 129–142.
- Drummond MS, Defant MJ, Kepezhinkas PK (1996). The petrogenesis of slab derived trondhjemite-tonalite-dacite/adakite magmas: *Transaction of the Royal Society of Edinburgh, Earth Sciences.* 87: 205-216.
- EI Sayed MM, Obeid MA, Furnes H, Moghazi AM(2004). Late Neoproterozoic volcanism in the southern Eastern Desert, Egypt: petrological, structural and geochemical constraints on the tectonic-magmatic evolution of the Allaqi Dokhan volcanic suite. *N. Jb. Miner. Abh.* 180(3): 261–286.
- EI-Desoky HM (2013). Geochemistry and Petrogenesis of Late Neoproterozoic Dokhan Volcanics at Wadi Abu Hamra area, Central Eastern Desert. *Egypt. J. Am Sci.* 9 (5): 212-235. (ISSN: 1545-1003). <http://www.jofamericanscience.org>. 28
- EI-Gaby S, Khudeir AA, El Taky M (1989). The Dokhan Volcanics of Wadi Queih area, central Eastern Desert, Egypt. In: *Proceedings of the 1st Conference on Geochemistry, Alexandria University, Egypt.* Pp. 42–62.
- EI-Gaby S, List FK, Tehrani R(1988). Geology, evolution and metallogenesis of the Pan-African belt in Egypt. In: EI Gaby, S., Greiling, R.O. (Eds.), *The Pan-African Belt of Northeast Africa and Adjacent Areas.* Braun, Schweig, Vieweg, Pp. 17–68.
- EI-Gaby S, List FK, Tehrani R(1990). The basement complex of the Eastern Desert and Sinai. In: Said, R. (Ed.). *The Geology of Egypt.* Balkema Rotterdam, The Netherlands. Pp. 175–184.
- EI-Gaby, S., 1975. Petrochemistry and geochemistry of some granites from Egypt. *N. Jb. Miner. Abh.* 124: 89–148.
- Eliwa HA, Kimura JI, Itaya T(2006). Late Neoproterozoic Dokhan Volcanics, North Eastern Desert, Egypt: geochemistry and petrogenesis. *Precamb. Res.* 151: 31–52.
- EI-Ramly MF (1972). A new geological map for the basement rocks in the eastern and southwestern deserts of Egypt. *Ann. Geol. Surv. Egypt.* 2: 1–18.
- EL-Ramly MF, Greiling RO, Kröner A, Rashwan A (1984). On the tectonic evolution of Wadi Hafafit area and environs, Eastern Desert of Egypt. *Bull Fac Sci King Abdulaziz Univ Jeddah.* 6:113–126
- Ewart A (1979). A review of the mineralogy and chemistry of the Tertiary- Recent dacitic, latitic, rhyolitic and related salic volcanic rocks. In: *Trondhjemites dacites and related rocks* (ed. BARKER, F.) Elsevier, Amsterdam. 13-121.
- Ewart A(1981). The mineralogy and petrology of Tertiary-Recent orogenic volcanic rocks: with special reference to the andesitic-basaltic compositional range. In: *Andesites* (ed. THORPE, J.) Elsevier, Amsterdam.
- Fitzsimons ICW (2000). Grenville-age basement provinces in East Antarctica: evidence for three separate collisional orogens. *Geology* 28: 879–882.

- Fritz H, Wallbrecher E, Khudeir AA, Abu El Ela FF, Dallmeyer DR (1996). Formation of Neoproterozoic metamorphic core complexes during oblique convergence Eastern Desert, Egypt. *J. Afr. Earth Sci.* 23: 311–329.
- Gass IG (1982). Upper Proterozoic (Pan-African) calc-alkaline magmatism in Northeastern Africa and Arabia. In: R.S. Thorpe (editor), *Andesites and related rocks*. Wiley and Sons, Chichester; New York. 591-609.
- Gill J (1981). *Orogenic Andesites and Plate Tectonics*. Springer, Berlin, Heidelberg, New York. Pp. 390.
- Greenberg JK (1981). Characteristics and origin of Egyptian younger granites. *Geol. Soc. Am. Bull.*, Prt II. 92: 749-840.
- Grothaus B, Eppler D, Ehrlich R(1979). Depositional environments and structural implications of the Hammamat Formation, Egypt. *Ann. Geol. Surv. Egypt* 9: 564–590.
- Gunnarsson B, Marsh BD, Taylor Jr HP (1998). Generation of Icelandic rhyolites: silicic lavas from the Torfajokull central volcano: *J. Volcano. Geothermal Res.* 83: 1-45.
- Halverson GP, Hurtgen MT, Porter SM, Collins AS (2009). Neoproterozoic–Cambrian biogeochemical evolution. In: Gaucher, C., Sial, A.N., Halverson, G.P., Frimmel, H.E. (Eds.), *Neoproterozoic–Cambrian Tectonics, Global Change and Evolution: a focus on southwestern Gondwana*. *Developments in Precambrian Geology*. Elsevier. Pp. 351–365.
- Hassan IS, Khalifa IH, Ibrahim SK (2001). Petrogenesis of late Precambrian Dokhan Volcanics suite at Wadi Meknas, southeastern Sinai, Egyptian. *J. Geol.* 45: 309–323.
- Hassan MA, Hashad AH (1990). Precambrian of Egypt. In: Said, R. (Ed.). *The Geology of Egypt*. Balkema, Rotterdam. Pp. 201–245.
- Hassanen MA (1997). Post-collision, A-type granites of Homrit Waggat complex, Egypt: petrological and geochemical constraints on its origin. *Precamb Res* 82: 211–236
- Heikal MA, Ahmed AM (1984). Late Precambrian volcanism in Gabal Abu Had, Eastern Desert-Egypt: Evidence for an island–arc environment. *Acta Mineralogica-Petrographica*, Szeged, 26(2): 221-233.
- Irvine TN, Baragar WRA (1971). A guide to the chemical classification of the common volcanic rocks. *Can. J. Earth. Sci.* 8: 523-548.
- Issawi B, Francis M, El-Hinnawy M, Mehanna A (1971). Geology of Safaga-Quseir coastal plain and Mahamed Rabah area. *Ann. Geol. Surv. Egypt*, Vol. I, P. 3-19.
- Jacobs J, Thomas RJ (2004). Himalayan-type indenter-escape tectonics model for the southern part of the late Neoproterozoic–early Paleozoic East African–Antarctic orogen. *Geology*. 32: 721–724.
- Jarrar G, Wachendorf H, Zachmann D (1993). A Pan-African alkaline pluton intruding the Saramuj conglomerate, south-west Jordan. *Geol. Rundsch.* 82: 121–135.
- Johnson K, Barnes CG, Miller CA (1997). Petrology, geochemistry, and genesis of high-Al tonalite and trondhjemites of the Cornucopia stock, Blue Mountains, Northeastern Oregon: *J. Petrology*. 38: 1585–1611.
- Kay RW (1978). Aleutian magnesian andesites: melts from subducted Pacific Ocean crust. *J. Volcan. Geotherm. Res.* 4: 117–132.
- Kay RW, Mahlburg-Kay S(1993). Delamination and delamination magmatism: *Tectonophysics*. 219(1-3): 177-189.
- Kröner A, Reischmann T, Wust HJ, Rashwan A (1988). Is there any pre-Pan-African (>950 Ma) basement in the Eastern Desert of Egypt? In: El Gaby, S., Greiling, R.O. (Eds.). *The Pan-African Belt of Northeast Africa and Adjacent Areas*. Vieweg, Braunschweig. Pp. 93–119.
- Kröner A, Todt W, Hussein IM, Mansour M, Rashwan A (1992). Dating of late Proterozoic ophiolites in Egypt and the Sudan using single zircon evaporation technique. *Precamb. Res.* 59: 15–32.
- Le Bas MJ, Le Maitre RW, Streckeisen A, Zanetin B (1986). A chemical classification of volcanic rocks based on the total alkalis-silica diagram. *J. Petrol.* 27: 745–750.
- Le Maitre RW (1989). *A Classification of Igneous Rocks and Glossary of Terms*. Blackwell, Oxford. Pp. 193.
- Maniar PA, Piccoli PM(1989). Tectonic discrimination of granitoids. *Bull. Geol. Soc. Am.* 101: 635-643.
- Martin H (1999). Adakitic magmas: modern analogues of Archean Granitoids. *Lithos* 26, 411–429.
- Martin H(1987). Petrogenesis of Archean trondhjemites, tonalities and granodiorites from eastern Finland: major and trace element geochemistry. *J. Petrol.* 28 (5):921–953.
- Martin H, Moyen JF (2003). Secular changes in TTG composition: comparison with modern adakites. In: EGS-AGU-EUG Joint Meeting, Nice, April, VGP7-1FR20-001.
- Martin H, Smithies RH, Rapp R, Moyen JF, Champion D (2005). An overview of adakite, tonalite–trondhjemite–granodiorites (TTG), and sanukitoid: relationships and some implications for crustal evolution. *Lithos*. 79: 1–24.
- Maury RC, Sajona FG, Pubellier M, Bellon H, Defant MJ (1996). Fusion de la croûte océanique dans les zones de subduction/collision récentes: l'exemple de Mindanao (Philippines). *Bull. Soc. Geol. Fr.* 167(5): 579–595.
- McDonough WF, Sun SS (1995). The composition of the Earth. *Chem. Geol.* 120: 223-253.
- Meert JG, Torsvik TH (2003). The making and unmaking of a supercontinent: Rodinia revisited. *Tectonophysics*. 375: 261–288.
- Meert JG, Van Der VR (1997). The assembly of Gondwana 800–550 Ma. *J. Geodynamics*. 23: 223–235.
- Meganck A (2004). Stratigraphy and petrology of volcanics from an abandoned tertiary rift, Langadalsfjall, Iceland: Seventeenth Annual Keck Research Symposium in Geology Proceedings, Washington and Lee University, Lexington, VA. pp. 135-138.
- Middlemost EAK (1985). *Magmas and magmatic rocks*. Longman, London.
- Miyashiro, A., 1973. The Troodos ophiolite complex was probably formed in an island arc. *Earth Planet. Sci. Lett.* 19: 218-224.
- Moghazi AM (1999). Magma source and evolution of late Neoproterozoic granitoids in the Gabal El Urf area, Eastern Desert, Egypt: geochemical and Sr–Nd isotopic constraints. *Geol. Mag.* 136: 285–300.
- Moghazi AM (2003). Geochemistry and petrogenesis of a high-K calc-alkaline Dokhan Volcanic suite, South Safaga area, Egypt: the role of late Neoproterozoic crustal extension. *Precambrian Research*. 125: 161–178.
- Mohamed FH, Moghazi AM, Hassanen MA (1999). Petrogenesis of late Proterozoic granitoids in the Ras Gharib magmatic province, northern Eastern Desert, Egypt: petrological and geochemical constraints. *N Jahrb Mineral Abh* 174: 319–353
- Mohamed FH, Moghazi AM, Hassanen MA (2000). Geochemistry, petrogenesis and tectonic setting of late Neoproterozoic Dokhan-type volcanic rocks in the Fatira area, eastern Egypt. *Int. J. Earth Sci.* 88: 764–777.
- Muir RJ, Weaver SD, Bradshaw JD, Eby GN, Evans JA(1995). Geochemistry of the Cretaceous Separation Point Batholith, New Zealand: granitoid magmas formed by melting of mafic lithosphere: *Journal of the Geological Society of London*. 152: 689–701.
- Pearce JA, Gale GH (1977). Identification of ore-deposition environment from trace element geochemistry of associated igneous host rocks. In: *Volcanic Processes in ore Genesis*. *Inst. Min. and Metallurgy, Geol. Soc. London, Spec. Publ.* 7: 14-24.
- Pearce TH, Gorman BE, Birkett TC (1977). The relationship between major element chemistry and tectonic environment of basic and intermediate volcanic rocks. *Earth Planet. Sci. Lett.* 36: 121-132.
- Pearce TH, Gorman BE, Birkett TC (1975). The TiO<sub>2</sub>-K<sub>2</sub>O-P<sub>2</sub>O<sub>5</sub> diagram: a method of discriminating between oceanic and non-oceanic basalts. *Earth Planet Sci. Lett.* 24: 419-426.
- Peccerillo A(1985). Roman comagmatic province (central Italy): evidence for subduction-related magma geneses. *Geology*. 13: 103–106.

- Petford N, Atherton MP (1996). Na-rich partial melts from newly underplated basaltic crust: the Cordillera Blanca Batholith, Peru. *J. Petrol.* 37: 1491–1521.
- Pisarevsky SA, Murphy JB, Cawood PA, Collins A.S., 2008. Late Neoproterozoic and Early Cambrian palaeogeography: models and problems. Geological Society, London, Special Publications 294, 9–31.
- Prouteau G, Scaillet B, Pichavant M, Maury RC (1999). Fluid-present melting of oceanic crust in subduction zones: *Geology*. 27: 1111–1114.
- Ragab AI (1987). On the petrogenesis of the Dokhan Volcanics of the Northern Eastern Desert of Egypt. *MERC Ain Shams Univ., Egypt, Earth Sci. Ser.* 1: 151–158.
- Rapp R, Watson E (1995). Dehydration melting of metabasalt at 8–32 kbar: Implications for continental growth and crust-mantle recycling: *J. Petrol.* 36(4): 891–931.
- Rapp RP, Xiao L, Shimizu N (2002). Experimental constraints on the origin of potassium-rich adakite in east China: *Acta Petrologica Sinica*. 18: 293–311.
- Rapp RP, Shimizu N, Norman MD, Applegate GS (1999). Reaction between slab-derived melts and peridotite in the mantle wedge: experimental constraints at 3.8 GPa. *Chem. Geol.* 160: 335–356.
- Rapp RP, Watson EB, Miller CF (1991). Partial melting of amphibolite/eclogite and the origin of Archaean trondhjemites and tonalites. *Precambrian Res.* 51: 1–25.
- Ressetar R, Monard JR (1983). Chemical composition and tectonic setting of the Dokhan Volcanic formation, Eastern Desert, Egypt. *J. Afr. Earth Sci.* 1: 103–112.
- Ries AC, Shackelton RM, Graham RH, Fitches WR (1983). Pan-African structures, ophiolites and melange in the Eastern Desert of Egypt: a traverse at 26°N. *J. Geol. Soc. Lond.* 140: 75–95.
- Rogers G, Saunders AD, Terrell DJ, Verma SP, Marriner GF (1985). Geochemistry of Holocene volcanic rocks associated with ridge subduction in Baja California, Mexico. *Nature*. 315: 389–392.
- Rogers NW, Hawkesworth CJ (1985). The geochemistry of potassic lavas from Vulsini, central Italy, and implications for mantle enrichment processes beneath the Roman region. *Contrib. Mineral. Petrol.* 90: 244–257.
- Rogers NW, Hawkesworth CJ, Mathey DP, Harmon RS (1987). Sediment subduction and the source of potassium in orogenic leucitites. *Geology*. 15: 451–453.
- Sabet AH (2010). Geology of some dolerite flows on the Red Sea Coast, south of El Quseir. *Egypt. J. Geol.* 2(1): 45–58.
- Sajona FG, Maury RC, Pubellier M, Leterrier J, Bellon H, Cotton J (2000). Magmatic source enrichment by slab-derived melts in a young post-collisional setting, central Mindanao (Philippines). *Lithos*. 54: 173–206.
- Saleh GM (2003). Neoproterozoic volcanism at Um Shilman-Um Dubr area, Southeast Aswan, Egypt: geology, geochemistry and tectonic environment of the Dokhan Volcanic Formation. *Neues Jahrbuch für Mineralogie. Abhandlungen*. 177: 321–347.
- Sen C, Dunn T (1994). Experimental modal metasomatism of a spinel lherzolite and the production of amphibole-bearing peridotite. *Contrib. Mineral. Petrol.* 119: 422–432.
- Sizova E, Gerya T, Brown M, Perchuk LL (2010). Subduction styles in the Precambrian: insight from numerical experiments. *Lithos*. 116: 209–229.
- Skjerlie KP, Patino-Douce AE (2002). The fluid-absent partial melting of a zoisite-bearing quartz eclogite from 1.0 to 3.2 GPa: implications for melting in thickened continental crust and for subduction-zone processes: *J. Petrol.* 43: 291–314.
- Slovan LE (1989). Triassic Shoshonites from the Dolomites, northern Italy, alkaline arc rocks in a strike-slip setting. *J. Geophys. Res.* 94: 4655–4666.
- Stern CR, Kilian R (1996). Role of the subducted slab, mantle wedge and continental crust in the generation of adakites from the Andean Austral Volcanic Zone. *Contrib. Miner. Petrol.* 123: 263–281.
- Stern RJ (1981). Petrogenesis and tectonic setting of Late Precambrian ensimatic volcanic rocks, central Eastern Desert of Egypt. *Precamb. Res.* 16: 195–230.
- Stern RJ (1994). Arc assembly and continental collision in the Neoproterozoic East African Orogen: implications for the consolidation of Gondwanaland. *Annual Review of Earth and Planetary Sciences*. 22: 319–351.
- Stern RJ (2002). Crustal evolution in the east African Orogen: a neodymium isotope perspective. *J. Afr. Earth Sci.* 34: 109–117.
- Stern RJ, Hedge CE (1985). Geochronologic and isotopic constraints on late Precambrian crustal evolution in the Eastern Desert of Egypt. *Am. J. Sci.* 285: 97–127.
- Stern RJ, Gottfried D, Hedge CE (1984). Late Precambrian rifting and crustal evolution in the northeast Desert of Egypt. *Geology*. 12: 168–172.
- Stern RJ, Johnson P (2010). Continental lithosphere of the Arabian Plate: a geologic, petrologic, and geophysical synthesis. *Earth Science Reviews*. 101: 29–67.
- Stern RJ, Sellers G, Gottfried D (1988). Bimodal dyke swarms in the North Eastern Desert of Egypt: significance for the origin of late Precambrian "A-type" granites in northern Afro-Arabia. In: El Gaby, S., Greiling, R.O. (Eds.), *The Pan-African Belt of Northeast Africa and Adjacent Areas*. Vieweg, Weisbaden. Pp. 147–177.
- Stern, R.J., Gottfried, D., 1986. Petrogenesis of late Precambrian (575–600 Ma) bimodal suite in northeast Africa. *Contrib. Mineral. Petrol.* 92, 492–501.
- Sturchio NC, Sultan M, Batiza R (1983). Geology and origin of Meatiq dome, Egypt: a Precambrian metamorphic core complex. *Geology*. 11: 72–76.
- Sylvester PJ (1989). Post-collisional alkaline granites. *J. Geol.* 97: 261–280.
- Taylor SR, McLennan SM (1985). The continental crust: its composition and evolution. *Geoscience Texts*. Blackwell Scientific Publishers, Oxford. Pp. 312.
- Thirwall MF (1988). Wenlock to mid-Devonian volcanism of the Caledonian–Applachian Orogen. In: Harris, A.I., Fettes, D.J. (Eds.), *The Caledonian–Applachian Orogen*. *Geol. Soc. London Spec. Publ.* 38: 415–428.
- Thomas RJ, De Waele B, Schofield DI, Goodenough KM, Horstwood M, Tucker RD, Bauer W, Annells R, Howard K, Walsh G, Rabarimanana M, Rafahatelo JM, Ralison AV, Randriamananjara T (2009). Geological evolution of the Neoproterozoic Bemarivo Belt, northern Madagascar. *Precambrian Research*. 172: 279–300.
- Tohver E, D'Agrella-Filho MS, Trindade RIF (2006). Paleomagnetic record of Africa and South America for the 1200–500 Ma interval, and evaluation of Rodinia and Gondwana assemblies. *Precambrian Research*. 147: 193–222.
- Tronnes RG (2002). Geology and geodynamics of Iceland: unpublished field guide, University of Iceland.
- Vail JR (1985). Pan-African (Late Precambrian) tectonic terrains and the reconstruction of the Arabian–Nubian Shield. *Geology*. 13: 839–842.
- Waston EB, Harrison TM (1983). Zircon saturation revisited: temperature and composition effects in a variety of crustal magma types. *Earth and Planetary Science Letters*. 64: 295–304.
- Watson EB (1979). Zircon saturation in felsic liquids: experimental results and applications to trace element geochemistry. *Contribution to Mineralogy and Petrology* 70: 407–419.
- Willis KM, Stern RJ, Clauer N (1988). Age and geochemistry of late Precambrian sediments of the Hammamat Series from the northeastern Desert of Egypt. *Precambrian Res.* 42: 173–187.
- Wilson M (1989). *Igneous petrogenesis*. Unwin Hyman, London.

Xiong XL, Li XH, Xu JF, Li WX, Zhao ZH, Wang Q, Chen XM (2003). Extremely high-Na adakite-like magmas derived from alkali-rich basaltic underplate: the Late Cretaceous Zhantang andesites in the Huichang Basin, SE China: *Geochemical J.* 37: 233–252.